The Beaker Phenomenon and the Genomic Transformation of Northwest Europe

Iñigo Olalde[1], Selina Brace[2], Morten E. Allentoft[3], Ian Armit[4,*], Kristian Kristiansen[5,*], Thomas Booth[2], Nadin Rohland[1], Swapan Mallick[1,6,7], Anna Szécsényi-Nagy[8], Alissa Mittnik[9,10], Eveline Altena[11], Mark Lipson[1], Iosif Lazaridis[1,6], Thomas K. Harper[12], Nick Patterson[6], Nasreen Broomandkhoshbacht[1,7], Yoan Diekmann[13], Zuzana Faltyskova[13], Daniel Fernandes[14,15,16], Matthew Ferry[1,7], Eadaoin Harney[1], Peter de Knijff[11], Megan Michel[1,7], Jonas Oppenheimer[1,7], Kristin Stewardson[1,7], Alistair Barclay[17], Kurt Werner Alt[18,19,20], Corina Liesau[21], Patricia Ríos[21], Concepción Blasco[21], Jorge Vega Miguel[22], Roberto Menduiña García[22], Azucena Avilés Fernández[23], Eszter Bánffy[24,25], Maria Bernabò-Brea[26], David Billoin[27], Clive Bonsall[28], Laura Bonsall[29], Tim Allen[30], Lindsey Büster[4], Sophie Carver[31], Laura Castells Navarro[4], Oliver E. Craig[32], Gordon T. Cook[33], Barry Cunliffe[34], Anthony Denaire[35], Kirsten Egging Dinwiddy[17], Natasha Dodwell[36], Michal Ernée[37], Christopher Evans[38], Milan Kuchařík[39], Joan Francès Farré[40], Harry Fokkens[41], Chris Fowler[42], Michiel Gazenbeek[43], Rafael Garrido Pena[21], María Haber-Uriarte[23], Elżbieta Haduch[44], Gill Hey[30], Nick Jowett[45], Timothy Knowles[46], Ken Massy[47], Saskia Pfrengle[9], Philippe Lefranc[48], Olivier Lemercier[49], Arnaud Lefebvre[50,51], César Heras Martínez[52,53,54], Virginia Galera Olmo[53,54], Ana Bastida Ramírez[52], Joaquín Lomba Maurandi[23], Tona Majó[55], Jacqueline I. McKinley[17], Kathleen McSweeney[28], Balázs Gusztáv Mende[8], Alessandra Modi[5]6, Gabriella Kulcsár[24], Viktória Kiss[24], András Czene[57], Róbert Patay[58], Anna Endrődi[59], Kitti Köhler[24], Tamás Hajdu[60,61], Tamás Szeniczey[60], János Dani[62], Zsolt Bernert[61], Maya Hoole[63], Olivia Cheronet[14,15], Denise Keating[64], Petr Velemínský[65], Miroslav Dobeš[37], Francesca Candilio[66,67,68], Fraser Brown[30], Raúl Flores Fernández[69], Ana-Mercedes Herrero-Corral[70], Sebastiano Tusa[71], Emiliano Carnieri[72], Luigi Lentini[73], Antonella Valenti[74], Alessandro Zanini[75], Clive Waddington[76], Germán Delibes[77], Elisa Guerra-Doce[77], Benjamin Neil[38], Marcus Brittain[38], Mike Luke[78], Richard Mortimer[36], Jocelyne Desideri[79], Marie Besse[79], Günter Brücken[80], Mirosław Furmanek[81], Agata Hałuszko[81], Maksym Mackiewicz[81], Artur Rapiński[82], Stephany Leach[83], Ignacio Soriano[84], Katina T. Lillios[85], João Luís Cardoso[86,87], Michael Parker Pearson[88], Piotr Włodarczak[89], T. Douglas Price[90], Pilar Prieto[91], Pierre-Jérôme Rey[92], Roberto Risch[84], Manuel A. Rojo Guerra[93], Aurore Schmitt[94], Joël Serralongue[95], Ana Maria Silva[96], Václav Smrčka[97], Luc Vergnaud[98], João Zilhão[86,99,100], David Caramelli[56], Thomas Higham[101], Mark G. Thomas[13], Philipp W. Stockhammer[47,102], Douglas J. Kennett[103], Volker Heyd[31,104], Alison Sheridan[105], Karl-Göran Sjögren[5], Johannes Krause[102], Ron Pinhasi[14,15,*], Wolfgang Haak[102,106,*], Ian Barnes[2,*], Carles Lalueza-Fox[107,*], David Reich[1,6,7,*]

*Principal investigators who contributed centrally to this study
To whom correspondence should be addressed: I.O. (inigo_olalde@hms.harvard.edu) or D.R. (reich@genetics.med.harvard.edu)

[1]Department of Genetics, Harvard Medical School, Boston, Massachusetts 02115, USA, [2]Department of Earth Sciences, Natural History Museum, London SW7 5BD, UK, [3]Centre for GeoGenetics, Natural History Museum, University of Copenhagen, Copenhagen 1350, Denmark, [4]School of Archaeological Sciences, University of Bradford, Bradford BD7 1DP, UK, [5]University of Gothenburg, Gothenburg 405 30, Sweden, [6]Broad Institute of MIT and Harvard, Cambridge, Massachusetts 02142, USA, [7]Howard Hughes Medical Institute, Harvard Medical School, Boston, Massachusetts 02115, USA, [8]Laboratory of Archaeogenetics, Institute of Archaeology, Research Centre for the Humanities, Hungarian Academy of Sciences, Budapest 1097, Hungary, [9]Institute for Archaeological Sciences, Archaeo- and Palaeogenetics, University of Tübingen, Tübingen 72070, Germany, [10]Department of Archaeogenetics, Max Planck Institute for the Science of Human History, 07745 Jena, Germany, [11]Department of Human Genetics, Leiden University Medical Center, Leiden 2333 ZC, The Netherlands, [12]Department of Anthropology, The Pennsylvania State University, University Park, PA 16802, USA, [13]Research Department of Genetics, Evolution and Environment, University College London, London WC1E 6BT, UK, [14]Earth Institute and School of Archaeology, University College Dublin, Dublin 4, Ireland, [15]Department of Anthropology, University of Vienna, Vienna 1090, Austria, [16]Research Center for Anthropology and Health, Department of Life Science, University of Coimbra, Coimbra 3000-456, Portugal, [17]Wessex Archaeology, Salisbury SP4 6EB, UK, [18]Center of Natural and Cultural History of Man, Danube Private University, Krems 3500, Austria, [19]Department of Biomedical Engineering, Basel University, Basel 4123, Switzerland, [20]Integrative Prehistory and Archaeological Science, Basel University, Switzerland, [21]Departamento de Prehistoria y Arqueología, Universidad Autónoma de Madrid, Madrid 28049, Spain, [22]ARGEA S.L., Madrid 28011, Spain, [23]Área de Prehistoria, Universidad de Murcia, Murcia 30001, Spain, [24]Institute of Archaeology, Research Centre for the Humanities, Hungarian Academy of Sciences, Budapest 1097, Hungary, [25]Romano-Germanic Commission, German Archaeological Institute, Frankfurt/Main 60325, Germany, [26]Museo Archeologico Nazionale di Parma, Parma 43100, Italy, [27]INRAP, Institut National de Recherches Archéologiques Préventives, Buffard 25440, France, [28]School of History, Classics and Archaeology, University of Edinburgh, Edinburgh EH8 9AG, UK, [29]Independent Researcher, 10 Merchiston Gardens, Edinburgh EH10 5DD, UK, [30]Oxford Archaeology, Oxford, OX2 0ES, UK, [31]Department of Archaeology and Anthropology, University of Bristol, Bristol BS8 1UU, UK, [32]BioArCh, Department of Archaeology, University of York, York YO10 5DD, UK, [33]Scottish Universities Environmental Research Centre East Kilbride G75 0QF, UK, [34]Institute of Archaeology, University of Oxford, Oxford OX1 2PG, UK, [35]University of Burgundy, Dijon 21000, France, [36]Oxford Archaeology East, Cambridge CB23 8SQ, UK, [37]Institute of Archaeology, Czech Academy of Sciences, Prague 118 01, Czech Republic, [38]Cambridge Archaeological Unit, Department of Archaeology, University of Cambridge, Cambridge CB3 0DT, UK, [39]Labrys o.p.s., Prague 198 00, Czech Republic, [40]Museu i Poblat Ibèric de Ca n'Oliver, Cerdanyola del Vallès 08290, Spain, [41]Faculty of Archaeology, Leiden University, 2333 CC Leiden, The Netherlands, [42]School of History, Classics & Archaeology, Newcastle University, Newcastle Upon Tyne NE1 7RU, UK, [43]INRAP, Institut National de Recherches Archéologiques Préventives, Nice 06300, France, [44]Institute of Zoology and

Biomedical Research, Jagiellonian University, Cracow 31-007, Poland, [45]Great Orme Mines, Great Orme, Llandudno LL30 2XG, UK, [46]Bristol Radiocarbon Accelerator Mass Spectrometry Facility, University of Bristol, Bristol BS8 1UU, UK, [47]Institut für Vor- und Frühgeschichtliche Archäologie und Provinzialrömische Archäologie, Ludwig-Maximilians-Universität München, Munich 80539, Germany, [48]INRAP, Institut National de Recherches Archéologiques Préventives, Strasbourg 67100, France, [49]Université Paul-Valéry - Montpellier 3, UMR 5140 ASM, Montpellier 34199, France, [50]INRAP, Institut National de Recherches Archéologiques Préventives, Metz 57063, France, [51]UMR 5199, Pacea, équipe A3P, Université de Bordeaux, Talence 33400, France, [52]TRÉBEDE, Patrimonio y Cultura SL, Torres de la Alameda 28813, Spain, [53]Departamento de Ciencias de la Vida, Universidad de Alcalá, Alcalá de Henares 28801, Spain, [54]Instituto Universitario de Investigación en Ciencias Policiales (IUICP), Alcalá de Henares 28801, Spain, [55]Archaeom. Departament de Prehistòria, Universitat Autònoma de Barcelona, Cerdanyola del Vallès 08193, Spain, [56]Department of Biology, University of Florence, Florence 50121, Italy, [57]Salisbury Ltd., Budaörs 2040, Hungary, [58]Ferenczy Museum Center, Szentendre 2100, Hungary, [59]Budapest History Museum, Budapest 1014, Hungary, [60]Department of Biological Anthropology, Eötvös Loránd University, Budapest 1117, Hungary, [61]Hungarian Natural History Museum, Budapest 1083, Hungary, [62]Déri Museum, Debrecen 4026, Hungary, [63]Historic Environment Scotland, Edinburgh EH9 1SH, UK, [64]Humanities Institute, University College Dublin, Dublin 4, Ireland, [65]Department of Anthropology, National Museum, Prague 115 79, Czech Republic, [66]Soprintendenza Archeologia belle arti e paesaggio per la città metropolitana di Cagliari e per le province di Oristano e Sud Sardegna, Cagliari 9124, Italy, [67]Physical Anthropology Section, University of Philadelphia Museum of Archaeology and Anthropology, Philadelphia, PA 19104, USA, [68]Department of Environmental Biology, Sapienza University of Rome, Rome 00185, Italy, [69]Professional archaeologist, [70]Departamento de Prehistoria, Universidad Complutense de Madrid, Madrid 28040, Spain, [71]Soprintendenza del Mare, Palermo 90133, Italia, [72]Facoltà di Lettere e Filosofia, Università di Palermo, Palermo 90133, Italy, [73]Soprintendenza per i beni culturali e ambientali di Trapani, Trapani 91100, Italy, [74]Prima Archeologia del Mediterraneo, Partanna 91028, Italy, [75]Università degli Studi di Palermo, Agrigento 92100, Italy, [76]Archaeological Research Services Ltd, Bakewell DE45 1HB, UK, [77]Departamento de Prehistoria, Facultad de Filosofía y Letras, Universidad de Valladolid, Valladolid 47011, Spain, [78]Albion Archaeology, Bedford MK42 0AS, UK, [79]Laboratory of Prehistoric Archaeology and Anthropology, Department F.-A. Forel for environmental and aquatic sciences, University of Geneva, Geneva 4, Switzerland, [80]General Department of Cultural Heritage Rhineland Palatinate, Department of Archaeology, Mainz 55116, Germany, [81]Institute of Archaeology, University of Wroclaw, Wrocław 50-137, Poland, [82]Institute of Archaeology, Silesian University in Opava, Opava 746 01, Czech Republic, [83]Department of Archaeology, University of Exeter, Exeter EX4 4QE, UK, [84]Departament de Prehistòria, Universitat Autònoma de Barcelona, Cerdanyola del Vallès 08193, Spain, [85]Department of Anthropology, University of Iowa, Iowa City, Iowa 52240, USA, [86]Centro de Arqueologia, Universidade de Lisboa, Lisboa 1600-214, Portugal, [87]Universidade Aberta, Lisboa 1269-001, Portugal, [88]Institute of Archaeology, University College London, London WC1H 0PY, UK, [89]Institute of Archaeology and Ethnology, Polish Academy of Sciences, Kraków 31-016, Poland, [90]Laboratory for Archaeological Chemistry, University of Wisconsin-Madison, Madison, Wisconsin 53706, USA, [91]University of Santiago de Compostela, Santiago de Compostela 15782, Spain, [92]UMR 5204 Laboratoire Edytem, Université Savoie Mont Blanc, Chambéry 73376, France, [93]Department of Prehistory and Archaeology, Faculty of Philosophy and Letters, Valladolid University, Valladolid 47011, Spain, [94]UMR 7268 ADES, CNRS, Aix-Marseille Univ, EFS, Faculté de médecine Nord, Marseille 13015, France, [95]Service archéologique, Conseil Général de la Haute-Savoie, Annecy 74000, France, [96]Laboratory of Prehistory, Research Center for Anthropology and Health, Department of Life Science, University of Coimbra, Coimbra 3000-456, Portugal, [97]Institute for History of Medicine and Foreign Languages, First Faculty of Medicine, Charles University, Prague 121 08, Czech Republic, [98]ANTEA Bureau d'étude en Archéologie, Habsheim 68440, France, [99]Institució Catalana de Recerca i Estudis Avançats, Barcelona 08010, Spain, [100]Departament d'Història i Arqueologia, Universitat de Barcelona, Barcelona 08001, Spain, [101]Oxford Radiocarbon Accelerator Unit, RLAHA, University of Oxford, Oxford OX1 3QY, UK, [102]Max Planck Institute for the Science of Human History, Jena 07745, Germany, [103]Department of Anthropology & Institute for Energy and the Environment, The Pennsylvania State University, University Park, PA 16802, USA, [104]Department of Philosophy, History, Culture and Art Studies, Section of Archaeology, University of Helsinki, Helsinki 00014, Finland, [105]National Museums Scotland, Edinburgh EH1 1JF, UK, [106]Australian Centre for Ancient DNA, School of Biological Sciences, University of Adelaide, Adelaide 5005, Australia, [107]Institute of Evolutionary Biology, CSIC-Universitat Pompeu Fabra, Barcelona 08003, Spain

Bell Beaker pottery spread across western and central Europe beginning around 2750 BCE before disappearing between 2200–1800 BCE. The forces propelling its expansion are a matter of long-standing debate, with support for both cultural diffusion and migration. We present new genome-wide data from 400 Neolithic, Copper Age and Bronze Age Europeans, including 226 Beaker-associated individuals. We detected limited genetic affinity between Iberian and central European Beaker-associated individuals, and thus exclude migration as a significant mechanism of spread between these two regions. However, migration played a key role in the further dissemination of the Beaker Complex, a phenomenon we document most clearly in Britain, where we report data from 155 individuals who lived from 4000-800 BCE. British Neolithic farmers were genetically similar to contemporary populations in continental Europe and especially to Neolithic Iberians, indicating that a portion of their ancestry came from the Mediterranean rather than the Danubian route of farming expansion. From the beginning of the Beaker period and onwards, all British individuals harboured high proportions of Steppe-related ancestry and were most closely related to Beaker-associated individuals from the Lower Rhine area. The impact of this migration from the continent was profound, as we show that the spread of the Beaker Complex to Britain was associated with a replacement of ~90% of Britain's gene pool within a few hundred years, continuing the east-to-west expansion that had brought Steppe-related ancestry into central and northern Europe 400 years earlier.

During the third millennium Before the Common Era (BCE), two new archaeological pottery styles expanded across Europe, replacing many of the more localized styles that preceded them.[1] The 'Corded Ware Complex' in north-central and northeastern Europe was associated with people who derived most of their ancestry from populations related to Early Bronze Age Yamnaya pastoralists from the Eurasian steppe[2–4] (henceforth referred to as Steppe). In western Europe there was the equally expansive 'Bell Beaker Complex', defined by assemblages of grave goods that included stylised bell-shaped pots, copper daggers, arrowheads, stone wristguards and V-perforated buttons[5] (Extended Data Fig. 1). The oldest radiocarbon dates associated with Beaker pottery are around 2750 BCE in Atlantic Iberia[6], which has been interpreted as evidence that the Beaker Complex originated there. However, the geographic origin is still debated[7] and other scenarios including an origin in the Lower Rhine area or even multiple independent origins are possible (Supplementary Information section 1). Regardless of the geographic origin, by 2500 BCE the Beaker Complex had spread throughout western Europe (and northwest Africa), and reached southern and Atlantic France, Italy and central Europe[5], where it overlapped geographically with the Corded Ware Complex. Within another hundred years, it had expanded to Britain and Ireland[8]. A major debate in archaeology has revolved around the question of whether the spread of the Beaker Complex was mediated by the movement of people, culture, or a combination of both[9]. Genome-wide data have revealed high proportions of Steppe-related ancestry in Beaker Complex-associated individuals from Germany and the Czech Republic[2–4], showing that they derived from mixtures of populations from the Steppe and the preceding Neolithic farmers of Europe. However, a deeper understanding of the ancestry of people associated with the Beaker Complex requires genomic characterization of individuals across the geographic range and temporal duration of this archaeological phenomenon.

Ancient DNA data

To understand the genetic structure of ancient people associated with the Beaker Complex and their relationship to preceding, subsequent and contemporary peoples, we used hybridization DNA capture[4,10] to enrich ancient DNA libraries for sequences overlapping 1,233,013 single nucleotide polymorphisms (SNPs), and generated new sequence data from 400 ancient Europeans dated to ~4700–800 BCE and excavated from 136 different sites (Extended Data Table 1; Supplementary Table 1; Supplementary Information, section 2). This dataset includes Beaker Complex-associated individuals from Iberia (n=37), southern France (n=4), northern Italy (n=3), Sicily (n=3), central Europe (n=133), The Netherlands (n=9) and Britain (n=37), and 174 individuals from other ancient populations, including 118 individuals from Britain who lived both before (n=51) and after (n=67) the arrival of the Beaker Complex (Fig. 1a-b). For genome-wide analyses, we filtered out first-degree relatives and individuals with low coverage (<10,000 SNPs) or evidence of DNA contamination (Methods) and combined our data with previously published ancient DNA data (Extended Data Fig. 2) to form a dataset of 683 ancient samples (Supplementary Table 1). We further merged these data with 2,572 present-day individuals genotyped on the Affymetrix Human Origins array[11,12] and 300 high coverage genomes[13]. To facilitate the interpretation of our genetic results, we also generated 111 new direct radiocarbon dates (Extended Data Table 2; Supplementary Information, section 3).

Y-chromosome analysis

The Y-chromosome composition of Beaker associated males was dominated by R1b-M269 (Supplementary Table 3), a lineage associated with the arrival of Steppe migrants in central Europe after 3000 BCE[2,3]. Outside Iberia, this lineage was present in 84 out of 90 analysed males. For individuals in whom we could determine the R1b-M269 subtype (n=60), we found that all but two had the derived allele for the R1b-S116/P312 polymorphism, which defines the dominant subtype in western Europe today[14]. In contrast, Beaker-associated individuals from the Iberian Peninsula carried a higher proportion of Y haplogroups known to be common across Europe during the earlier Neolithic period[2,4,15,16], such as I (n=5) and G2 (n=1), while R1b-

M269 was found in four individuals with a genome-wide signal of Steppe-related ancestry (the two with higher coverage could be further classified as R1b-S116/P312). Finding this widespread presence of the R1b-S116/P312 polymorphism in ancient individuals from central and western Europe suggests that people associated with the Beaker Complex may have had an important role in the dissemination of this lineage throughout most of its present-day distribution.

Genomic insights into the spread of people associated with the Beaker Complex

We performed Principal Component Analysis (PCA) by projecting the ancient samples onto a set of west Eurasian present-day populations. We replicated previous findings[11] of two parallel clines, with present-day Europeans on one side and present-day Near Easterners on the other (Extended Data Fig. 3a). Individuals associated with the Beaker Complex are strikingly heterogeneous within the European cline—splayed out along the axis of variation defined by Early Bronze Age Yamnaya individuals from the Steppe at one extreme and Middle Neolithic/Copper Age Europeans at the other extreme (Fig. 1c; Extended Data Fig. 3a)—suggesting that the genetic differentiation may be related to variable amounts of Steppe-related ancestry. We obtained qualitatively consistent inferences using ADMIXTURE model-based clustering[17]. Beaker Complex-associated individuals harboured three main genetic components: one characteristic of European Mesolithic hunter-gatherers, one maximized in Neolithic individuals from the Levant and Anatolia, and one maximized in Neolithic individuals of Iran and present in admixed form in Steppe populations (Extended Data Fig. 3b).

Both PCA and ADMIXTURE are powerful tools for visualizing genetic structure but they do not provide formal tests of admixture between populations. We grouped Beaker Complex individuals based on geographic proximity and genetic similarity (Supplementary Information, section 6), and used *qpAdm*[2] to directly test admixture models and estimate mixture proportions. We modelled their ancestry as a mixture of Mesolithic western European hunter-gatherers (WHG), northwestern Anatolian Neolithic farmers, and Early Bronze Age Steppe populations (the first two of which contributed to earlier Neolithic Europeans; Supplementary Information, section 8). We find that the great majority of sampled Beaker Complex individuals in areas outside of Iberia (with the exception of Sicily) derive a large portion of their ancestry from Steppe populations(Fig. 2a), whereas in Iberia, such ancestry is present in only eight of the 32 analysed individuals, who represent the earliest detection of Steppe-related genomic affinities in this region. We observe striking differences in ancestry not only at a pan-European scale, but also within regions and even within sites. Unlike other individuals from the Upper Alsace region of France (n=2), an individual from Hégenheim resembles the previous Neolithic populations and can be modelled as a mixture of Anatolian Neolithic and western hunter-gatherers without any Steppe-related ancestry. Given that the radiocarbon date of the Hégenheim individual is older (2832–2476 cal BCE; all dates quoted as 95.4% confidence intervals; Supplementary Information, section 2) than other samples from the same region (2566–2133 cal BCE), the pattern could reflect temporal differentiation. At Szigetszentmiklós in Hungary, we find roughly contemporary Beaker-associated individuals with very different proportions (from 0% to 75%) of Steppe-related ancestry. This genetic heterogeneity is consistent with early stages of mixture between previously established European Neolithic populations and migrants with Steppe-related ancestry. An implication is that, even at a local scale, the Beaker Complex was associated with people of diverse ancestries.

While the Steppe-related ancestry in Beaker-associated individuals had a recent origin in the East[2,3], the other ancestry component (from previously established European populations) could potentially be derived from several parts of Europe, as genetically closely related groups were widely distributed during the Neolithic and Copper Ages[2,4,11,16,18–23]. To obtain insight into the origin of this ancestry component in Beaker Complex-associated individuals, we looked for regional patterns of genetic differentiation within Europe during the Neolithic and Copper Age periods. We examined whether Neolithic and Copper Age test populations predating the emergence of the Beaker Complex shared more alleles with Iberian (*Iberia_EN*) or central European Linearbandkeramik (*LBK_EN*) Early Neolithic populations. As previously described[2], there is genetic affinity to Iberian Early Neolithic farmers in Iberian Middle Neolithic/Copper Age populations, but not in central and northern European Neolithic populations (Fig. 2b). These regional patterns could be partially explained by differential genetic affinities to pre-Neolithic hunter-gatherer individuals from different regions[22] (Extended Data Fig. 4). Neolithic individuals from southern France and Britain are also significantly closer to Iberian Early Neolithic farmers than to central European Early Neolithic farmers (Fig. 2b), consistent with the analysis of a Neolithic genome from Ireland[23]. By modelling Neolithic populations and WHG in an admixture graph framework, we replicate these results and further show that they are not driven by different proportions of hunter-gatherer admixture (Extended Data Fig. 5; Supplementary Information, section 7). Our results suggest that a portion of the ancestry of the Neolithic populations of Britain was derived from migrants who spread along the Atlantic coast. Megalithic tombs document substantial interaction along the Atlantic façade of Europe, and our results are consistent with such interactions reflecting south-to-north movements of people. More data from southern Britain and Ireland (where currently data are sparse) and nearby regions in continental Europe will be needed to fully understand the complex interactions between Britain, Ireland, and the continent during the Neolithic[24].

The distinctive genetic signatures of pre-Beaker Complex populations in Iberia compared to central Europe allow us to test formally for the origin of the Neolithic-related ancestry in Beaker

Complex-associated individuals in our dataset (Supplementary Information, section 8). We grouped individuals from Iberia (n=32) and from outside Iberia (n=172) to increase power, and evaluated the fit of different Neolithic/Copper Age groups with *qpAdm* under the model: Steppe_EBA + Neolithic/Copper Age. For Beaker Complex-associated individuals from Iberia, the best fit was obtained when Middle Neolithic and Copper Age populations from the same region were used as the source for their Neolithic-related ancestry, and we could exclude central and northern European populations ($P < 0.0063$) (Fig. 2c). Conversely, the Neolithic-related ancestry in Beaker Complex individuals outside Iberia was most closely related to central and northern European Neolithic populations with relatively high hunter-gatherer admixture (e.g. *Poland_LN*, $P = 0.18$; *Sweden_MN*, $P = 0.25$), and we could significantly exclude Iberian sources ($P < 0.0104$) (Fig. 2c). These results support largely different origins for Beaker Complex-associated individuals, with no discernible Iberia-related ancestry outside Iberia.

Nearly complete turnover of ancestry in Britain

British Beaker Complex-associated individuals (n=37) show strong similarities to central European Beaker Complex-associated individuals in their genetic profile (Extended Data Fig. 3). This observation is not restricted to British individuals associated with the 'All-Over-Cord' Beaker pottery style that is shared between Britain and Central Europe, as we also find this genetic signal in British individuals associated with Beaker pottery styles derived from the 'Maritime' forms that were the predominant early style in Iberia. The presence of large amounts of Steppe-related ancestry in British Beaker Complex-associated individuals (Fig. 2a) contrasts sharply with Neolithic individuals from Britain (n=51), who have no evidence of Steppe genetic affinities and cluster instead with Middle Neolithic and Copper-Age populations from mainland Europe (Extended Data Fig. 3). Thus, the arrival of Steppe-related ancestry in Britain was mediated by a migration that began with the Beaker Complex. A previous study showed that Steppe-related ancestry arrived in Ireland by the Bronze Age[23], and here we show that – at least in Britain – it arrived earlier in the Copper Age/Beaker period.

Among the different continental Beaker Complex groups analysed in our dataset, individuals from Oostwoud (Province of Noord-Holland, The Netherlands) are the most closely related to the great majority of the Beaker Complex individuals from southern Britain (n=27). The two groups had almost identical Steppe-related ancestry proportions (Fig. 2a), the highest level of shared genetic drift (Extended Data Fig. 6b), and were symmetrically related to most ancient populations (Extended Data Fig. 6a), showing that they are likely derived from the same ancestral population with limited mixture into either group. This does not necessarily imply that the Oostwoud individuals are direct ancestors of the British individuals. However, it shows that they were genetically closely-related to the population (perhaps yet to be sampled) that moved into Britain from continental Europe.

We investigated the magnitude of population replacement in Britain with *qpAdm,*[2] modelling the genome-wide ancestry of Neolithic, Copper and Bronze Age individuals (including Beaker Complex-associated individuals) as a mixture of continental Beaker Complex-associated samples (using the Oostwoud individuals as a surrogate) and the British Neolithic population (Supplementary Information, section 8). During the first centuries after the initial contact (between ~2450–2000 BCE), ancestry proportions were variable (Fig. 3), consistent with migrant communities that were just beginning to mix with the previously established Neolithic population of Britain. After ~2000 BCE, individuals were more homogeneous, with less variation in ancestry proportions and a modest increase in Neolithic-related ancestry (Fig. 3), which could represent admixture with persisting British populations with high levels of Neolithic-related ancestry (or alternatively incoming continental populations with higher proportions of Neolithic-related ancestry). In either case, our results imply a minimum of 90±2% local population turnover by the Middle Bronze Age (~1500–1000 BCE), with no significant decrease observed in 5 samples from the Late Bronze Age (Supplementary Information, section 8). While the exact turnover rate and its geographic pattern will be refined with further ancient samples, our results imply that for individuals from Britain during and after the Beaker period, a very high fraction of their DNA derives from ancestors who lived in continental Europe prior to 2450 BCE. An independent line of evidence for population turnover comes from Y-chromosome haplogroup composition. While R1b haplogroups were completely absent in Neolithic individuals (n=33), they represent more than 90% of the Y-chromosomes during Copper and Bronze Age Britain (n=52) (Fig. 3; Supplementary Table 3).

Our genetic time transect in Britain also allowed us to track the frequencies of alleles with known phenotypic effects. Derived alleles at rs16891982 (SLC45A2) and rs12913832 (HERC2/OCA2), which contribute to reduced skin and eye pigmentation in Europeans, dramatically increased in frequency between the Neolithic period and the Beaker and Bronze Age periods (Extended Data Fig. 7). Thus, the arrival of migrants associated with the Beaker Complex significantly altered the pigmentation phenotypes of British populations. However, the lactase persistence allele at SNP rs4988235 remained at very low frequencies across this transition, both in Britain and continental Europe, showing that the major increase in its frequency in Britain, as in mainland Europe[3,4,25], occurred in the last 3,500 years.

Discussion

The term 'Bell Beaker' was introduced by late 19th-century and early 20th-century archaeologists to refer to the distinctive pottery style found across western and central Europe at the end of the Neolithic, initially hypothesized to have been spread by a genetically homogeneous group of people. This idea of a 'Beaker Folk' became unpopular after the 1960s as scepticism grew about the role of migration in mediating change in archaeological cultures[26], although J.G.D. Clark speculated that the Beaker Complex expansion into Britain was an exception[27], a prediction that has now been borne out by ancient genomic data.

Our results prove that the expansion of the Beaker Complex cannot be described by a simple one-to-one mapping of an archaeologically defined material culture to a genetically homogeneous population. This stands in contrast to other archaeological complexes genetically analysed to date, notably the *Linearbandkeramik* first farmers of central Europe[2], the Early Bronze Age Yamnaya of the Steppe[2,3], and to some extent the Corded Ware Complex of central and eastern Europe[2,3]. Instead, our results support a model in which cultural transmission and human migration both played important roles, with the relative balance of these two processes depending on the region. In Iberia, the majority of Beaker-associated individuals lacked Steppe affinities and were genetically most similar to preceding Iberian populations. In central Europe, Steppe-related ancestry was widespread and we can exclude a substantial contribution from Iberian Beaker associated individuals, contradicting initial suggestions of gene flow into central Europe based on analysis of mtDNA[28] and dental morphology[29]. The presence of Steppe-related ancestry in some Iberian individuals demonstrates that gene-flow into Iberia was, however, not uncommon during this period.

In other parts of Europe, the Beaker Complex expansion was driven to a substantial extent by migration. This genomic transformation is clearest in Britain due to our densely sampled time transect. The arrival of people associated with the Beaker Complex precipitated a profound demographic transformation in Britain, exemplified by the presence of individuals with large amounts of Steppe-related ancestry after 2450 BCE. We considered the possibility that an uneven geographic distribution of samples could have caused us to miss a major population lacking Steppe-derived ancestry after 2450 BCE. However, our British Beaker and Bronze Age samples are dispersed geographically, extending from England's southeastern peninsula to the Western Isles of Scotland, and come from a wide variety of funerary contexts (rivers, caves, pits, barrows, cists and flat graves) and diverse funerary traditions (single and multiple burials in variable states of anatomical articulation), reducing the likelihood that our sampling missed major populations. We also considered the possibility that different burial practices between local and incoming populations (cremation versus inhumation) during the early stages of interaction, could result in a sampling bias against local individuals. While it is possible that such a sampling bias makes the ancestry transition appear more sudden than it in fact was, the long-term demographic impact was clearly profound, as the pervasive Steppe-related ancestry observed during the Copper Age/Beaker period and absent in the Neolithic persisted among the

67 Bronze Age individuals we report here, and indeed remains predominant in Britain today[2]. These results are notable in light of strontium and oxygen isotope analyses of British skeletons from the Beaker and Bronze Age periods[30], which have provided no evidence of substantial mobility over individuals' lifetimes from locations with cooler climates or from places with geologies atypical of Britain. However, the isotope data are only sensitive to first-generation migrants and do not rule out movements from regions such as the lower Rhine area, which is consistent with the genetic data, or from other geologically similar regions for which DNA sampling is still sparse. Further sampling of regions on the European continent may reveal additional candidate sources.

By analysing DNA data from ancient individuals, we have been able to provide constraints on the interpretations of the processes underlying cultural and social changes in Europe during the third millennium BCE. Our results motivate further archaeological research to identify the changes in social organization, technology, subsistence, climate, population sizes[31] or pathogen exposure[32,33] that could have precipitated the demographic changes uncovered in this study.

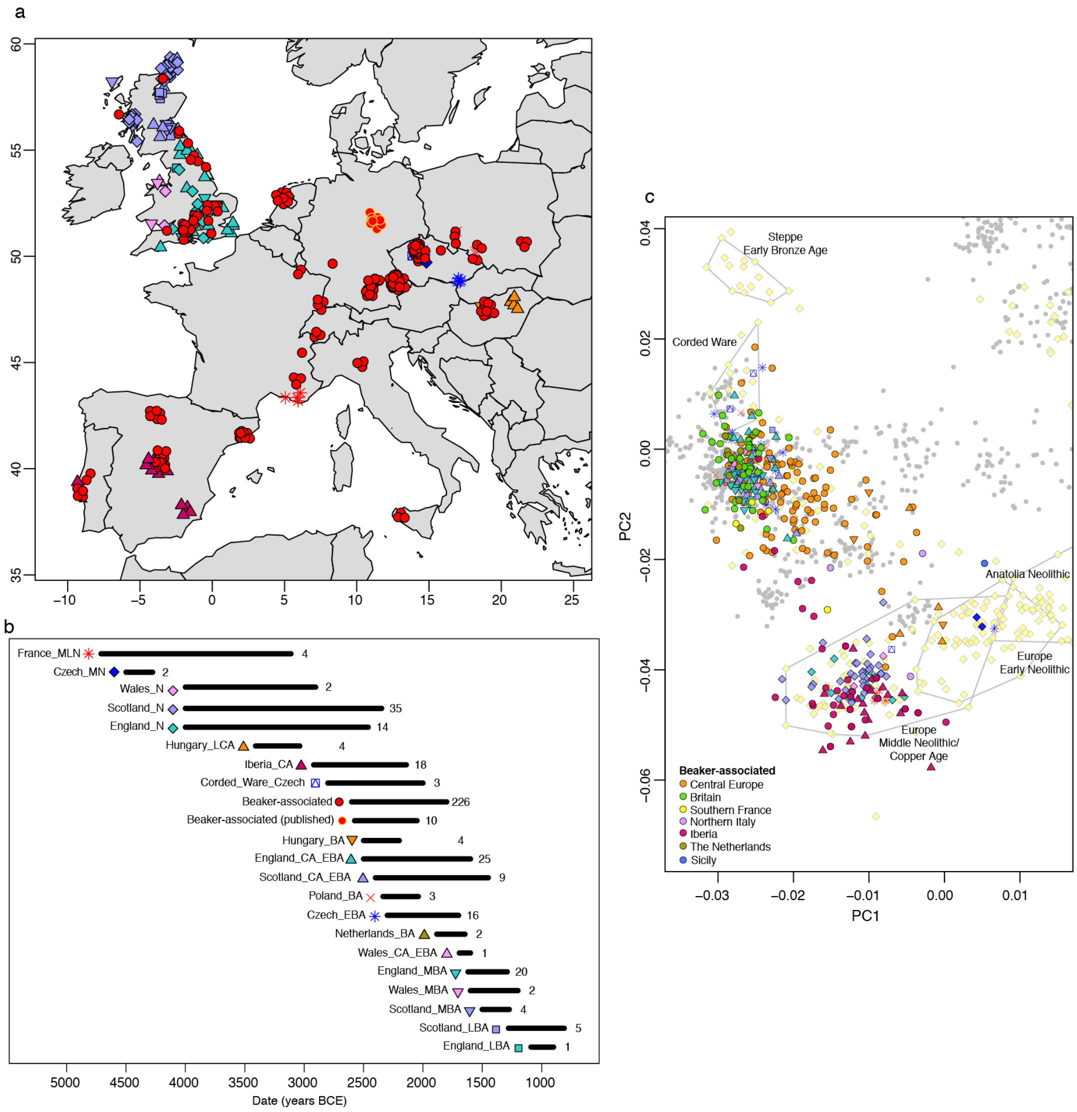

Figure 1. Spatial, temporal, and genetic structure of individuals in this study. a, Geographic distribution of samples with new genome-wide data. For clarity, random jitter was added for sites with multiple individuals. **b**, Approximate time ranges for samples with new genome-wide data. Sample sizes are given next to each bar. **c**, Principal component analysis of 990 present-day West Eurasian individuals (grey dots), with previously published (pale yellow) and new ancient samples projected onto the first two principal components. This figure is a zoom of Extended Data Fig 3a. E, Early; M, Middle; L, Late; N, Neolithic; CA, Copper Age; BA, Bronze Age.

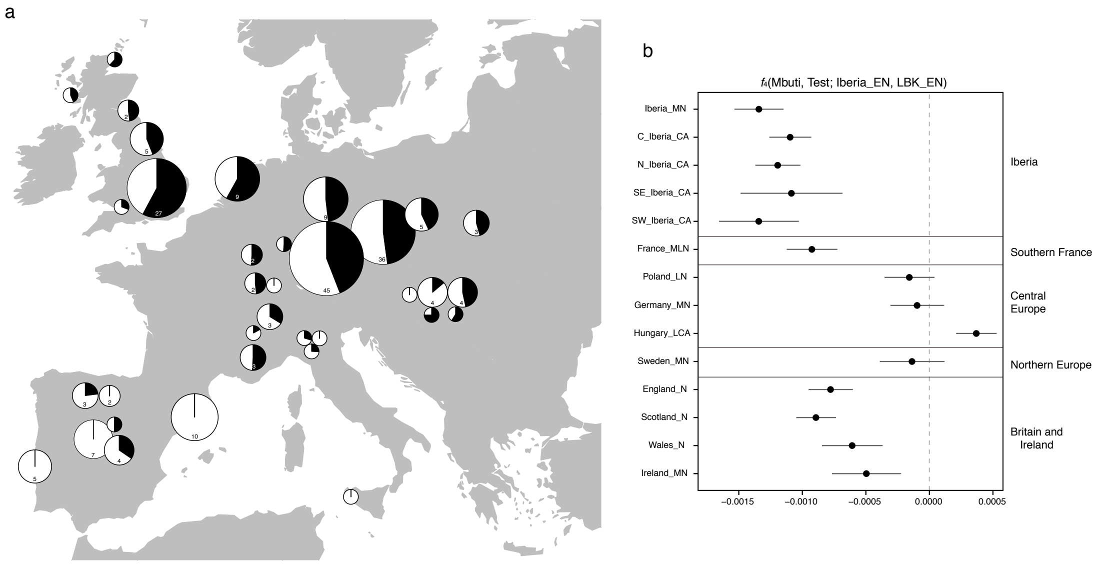

c

		Neolithic/Copper Age source pop									
		Iberia_MN	C_Iberia_CA	N_Iberia_CA	SE_Iberia_CA	SW_Iberia_CA	Germany_MN	Poland_LN	Hungary_LCA	Sweden_MN	France_MLN
Test pop	BC Iberia combined	1.66E-01	7.23E-01	1.76E-05	1.15E-01	6.11E-01	8.17E-11	3.36E-06	2.72E-59	6.28E-03	4.53E-02
	BC outside Iberia combined	1.11E-12	7.48E-10	2.18E-10	9.93E-03	1.04E-02	2.51E-13	1.84E-01	6.05E-55	2.45E-01	4.61E-04

Figure 2. Investigating the genetic makeup of Beaker Complex individuals. a, Proportion of Steppe-related ancestry (shown in black) in Beaker Complex-associated groups, computed with *qpAdm* under the model Steppe_EBA + Anatolia_N + WHG. The area of the pie is proportional to the number of individuals (shown inside the pie if more than one). See Supplementary Information, section 8 for mixture proportions and standard errors. **b**, *f*-statistics of the form f_4(Mbuti, *Test*; Iberia_EN, LBK_EN) computed for European populations before the emergence of the Beaker Complex. The statistic takes negative values if the *Test* shares more alleles with Iberia_EN (positive values in the case of excess affinity with LBK_EN). Error bars represent ±1 standard errors. **c**, Testing different populations as a source for the Neolithic ancestry component in Beaker Complex individuals. The table shows the P-values (highlighted if >0.05) for the model: Steppe_EBA + Neolithic/Copper Age source population. BC, Beaker complex; E, Early; M, Middle; L, Late; N, Neolithic; CA, Copper Age; BA, Bronze Age; N_Iberia, Northern Iberia; C_Iberia, Central Iberia; SE_Iberia, Southeast Iberia; SW_Iberia, Southwest Iberia.

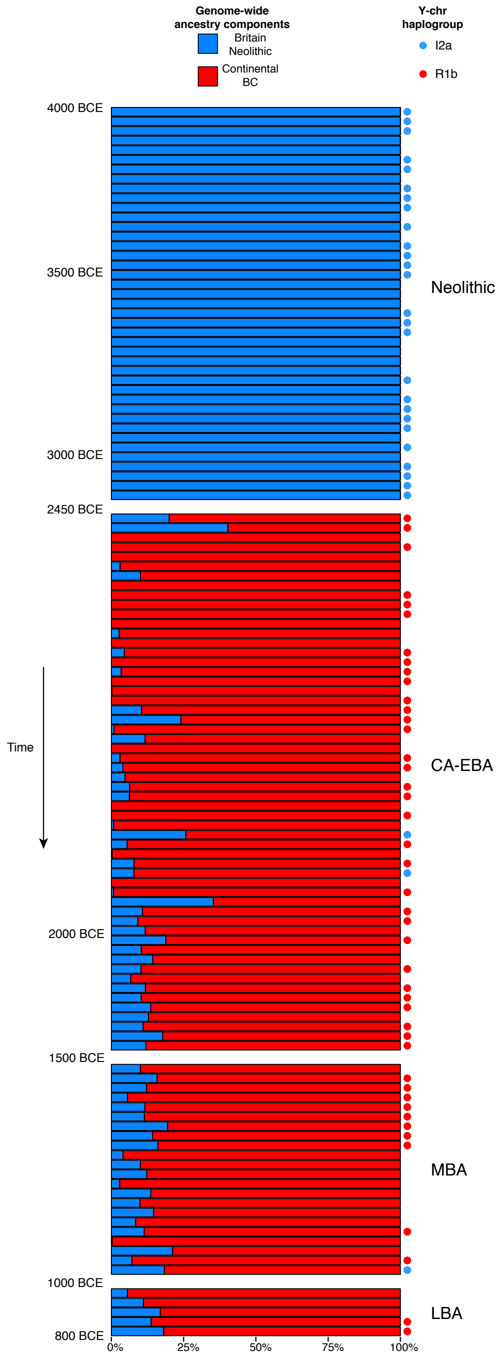

Figure 3. Population transformation in Britain associated with the arrival of the Beaker Complex. Modelling Neolithic, Copper and Bronze Age (including Beaker Complex-associated) individuals from Britain as a mixture of continental Beaker Complex-associated individuals (red) and the Neolithic population from Britain (blue). Each bar represents genome-wide mixture proportions for one individual. Individuals are ordered chronologically (oldest on the top) and included in the plot if represented by more than 100,000 SNPs. See Supplementary Information, section 8 for mixture proportions and standard errors. Circles indicate the Y-chromosome haplogroup for male individuals. CA, Copper Age; EBA, Early Bronze Age; MBA, Middle Bronze Age; LBA, Late Bronze Age. BC, Beaker complex**.**

References

1. Czebreszuk, J. Bell Beakers from West to East. In *Ancient Europe, 8000 B.C. to A.D. 1000: An Encyclopedia of the Barbarian World* (eds. Bogucki, P. I. & Crabtree, P. J.) 476–485 (Charles Scribner's Sons, 2004).
2. Haak, W. *et al.* Massive migration from the steppe was a source for Indo-European languages in Europe. *Nature* **522,** 207–211 (2015).
3. Allentoft, M. E. *et al.* Population genomics of Bronze Age Eurasia. *Nature* **522,** 167–172 (2015).
4. Mathieson, I. *et al.* Genome-wide patterns of selection in 230 ancient Eurasians. *Nature* **528,** 499–503 (2015).
5. Czebreszuk, J. Similar But Different. Bell Beakers in Europe. *Adam Mickiewicz University* (2004).
6. Cardoso, J. L. Absolute chronology of the Beaker phenomenon North of the Tagus estuary : demographic and social implications. *Trabajos de Prehistoria* **71,** 56–75 (2014).
7. Jeunesse, C. The dogma of the Iberian origin of the Bell Beaker: attempting its deconstruction. *J. Neolit. Archaeol.* **16,** 158–166 (2015).
8. Fokkens, H. & Nicolis, F. *Background to Beakers. Inquiries into regional cultural backgrounds of the Bell Beaker complex*. (Leiden: Sidestone Press, 2012).
9. Vander Linden, M. What linked the Bell Beakers in third millennium BC Europe? *Antiquity* **81,** 343–352 (2007).
10. Fu, Q. *et al.* An early modern human from Romania with a recent Neanderthal ancestor. *Nature* **524,** 216–219 (2015).
11. Lazaridis, I. *et al.* Ancient human genomes suggest three ancestral populations for present-day Europeans. *Nature* **513,** 409–413 (2014).
12. Lazaridis, I. *et al.* Genomic insights into the origin of farming in the ancient Near East. *Nature* **536,** 1–22 (2016).
13. Mallick, S. *et al.* The Simons Genome Diversity Project: 300 genomes from 142 diverse populations. *Nature* **538,** (2016).
14. Valverde, L. *et al.* New clues to the evolutionary history of the main European paternal lineage M269: dissection of the Y-SNP S116 in Atlantic Europe and Iberia. *Eur. J. Hum. Genet.* 1–5 (2015). doi:10.1038/ejhg.2015.114
15. Gamba, C. *et al.* Ancient DNA from an Early Neolithic Iberian population supports a pioneer colonization by first farmers. *Mol. Ecol.* **21,** 45–56 (2012).
16. Günther, T. *et al.* Ancient genomes link early farmers from Atapuerca in Spain to modern-day Basques. *Proc. Natl. Acad. Sci. U. S. A.* **112,** 11917–11922 (2015).
17. Alexander, D. H., Novembre, J. & Lange, K. Fast model-based estimation of ancestry in unrelated individuals. *Genome Res.* **19,** 1655–1664 (2009).
18. Broushaki, F. *et al.* Early Neolithic genomes from the eastern Fertile Crescent. *Science* **7943,** 1–16 (2016).
19. Skoglund, P. *et al.* Genomic Diversity and Admixture Differs for Stone-Age Scandinavian Foragers and Farmers. *Science* **201,** 786–792 (2014).
20. Olalde, I. *et al.* A Common Genetic Origin for Early Farmers from Mediterranean Cardial and Central European LBK Cultures. *Mol. Biol. Evol.* **32,** 3132–3142 (2015).
21. Mathieson, I. *et al.* The Genomic History of Southeastern Europe. *bioRxiv* (2017).
22. Lipson, M. *et al.* Parallel ancient genomic transects reveal complex population history of early European farmers. *bioRxiv* (2017).
23. Cassidy, L. M. *et al.* Neolithic and Bronze Age migration to Ireland and establishment of the insular Atlantic genome. *Proc. Natl. Acad. Sci. U. S. A.* **113,** 1–6 (2016).
24. Sheridan, J. A. The Neolithisation of Britain and Ireland: the big picture. In *Landscapes in transition* (eds. Finlayson, B. & Warren, G.) 89–105 (Oxbow, Oxford, 2010).
25. Burger, J., Kirchner, M., Bramanti, B., Haak, W. & Thomas, M. G. Absence of the lactase-persistence-associated allele in early Neolithic Europeans. *Proc. Natl. Acad. Sci. U. S. A.* **104,** 3736–41 (2007).
26. Clarke, D. L. The Beaker network: social and economic models. in *Glockenbecher*

Symposion,Oberried, 18–23 März 1974 (eds. Lanting, J. N. & DerWaals, J. D. van) 460–77 (1976).
27. Clark, G. The Invasion Hypothesis in British Archaeology. *Antiquity* **40,** 172–189 (1966).
28. Brotherton, P. *et al.* Neolithic mitochondrial haplogroup H genomes and the genetic origins of Europeans. *Nat. Commun.* **4,** 1764 (2013).
29. Desideri, J. When Beakers Met Bell Beakers : an analysis of dental remains. *British archaeological Reports - International Series; 2292* (2011).
30. Parker Pearson, M. *et al.* Beaker people in Britain: migration, mobility and diet. *Antiquity* **90,** 620–637 (2016).
31. Shennan, S. *et al.* Regional population collapse followed initial agriculture booms in mid-Holocene Europe. *Nat. Commun.* **4,** 2486 (2013).
32. Valtueña, A. A. *et al.* The Stone Age Plague : 1000 years of Persistence in Eurasia. *bioRxiv* (2016).
33. Rasmussen, S. *et al.* Early Divergent Strains of Yersinia pestis in Eurasia 5,000 Years Ago. *Cell* **163,** 571–582 (2015).
34. Dabney, J. *et al.* Complete mitochondrial genome sequence of a Middle Pleistocene cave bear reconstructed from ultrashort DNA fragments. *Proc. Natl. Acad. Sci. U. S. A.* **110,** 15758–63 (2013).
35. Damgaard, P. B. *et al.* Improving access to endogenous DNA in ancient bones and teeth. *Sci. Rep.* **5,** 11184 (2015).
36. Korlević, P. *et al.* Reducing microbial and human contamination in dna extractions from ancient bones and teeth. *Biotechniques* **59,** 87–93 (2015).
37. Rohland, N., Harney, E., Mallick, S., Nordenfelt, S. & Reich, D. Partial uracil – DNA – glycosylase treatment for screening of ancient DNA. *Philos. Trans. R. Soc. London B* **370**:20130624 (2015).
38. Briggs, A. W. *et al.* Removal of deaminated cytosines and detection of in vivo methylation in ancient DNA. *Nucleic Acids Res.* **38,** 1–12 (2010).
39. Maricic, T., Whitten, M. & Pääbo, S. Multiplexed DNA sequence capture of mitochondrial genomes using PCR products. *PLoS One* **5,** e14004 (2010).
40. Kircher, M., Sawyer, S. & Meyer, M. Double indexing overcomes inaccuracies in multiplex sequencing on the Illumina platform. *Nucleic Acids Res.* **40,** 1–8 (2012).
41. Behar, D. M. *et al.* A 'Copernican' reassessment of the human mitochondrial DNA tree from its root. *Am. J. Hum. Genet.* **90,** 675–84 (2012).
42. Li, H. & Durbin, R. Fast and accurate short read alignment with Burrows–Wheeler transform. *Bioinformatics* **25,** 1754–1760 (2009).
43. Fu, Q. *et al.* A revised timescale for human evolution based on ancient mitochondrial genomes. *Curr. Biol.* **23,** 553–9 (2013).
44. Sawyer, S., Krause, J., Guschanski, K., Savolainen, V. & Pääbo, S. Temporal patterns of nucleotide misincorporations and DNA fragmentation in ancient DNA. *PLoS One* **7,** e34131 (2012).
45. Korneliussen, T. S., Albrechtsen, A. & Nielsen, R. ANGSD : Analysis of Next Generation Sequencing Data. *BMC Bioinformatics* **15,** 1–13 (2014).
46. Li, H. *et al.* The Sequence Alignment/Map format and SAMtools. *Bioinformatics* **25,** 2078–9 (2009).
47. Weissensteiner, H. *et al.* HaploGrep 2: mitochondrial haplogroup classification in the era of high-throughput sequencing. *Nucleic Acids Res.* **44,** W58-63 (2016).
48. van Oven, M. & Kayser, M. Updated comprehensive phylogenetic tree of global human mitochondrial DNA variation. *Hum. Mutat.* **30,** E386-94 (2009).
49. Patterson, N. *et al.* Ancient admixture in human history. *Genetics* **192,** 1065–93 (2012).
50. Raghavan, M. *et al.* Upper Palaeolithic Siberian genome reveals dual ancestry of Native Americans. *Nature* **505,** 87–91 (2014).
51. Omrak, A. *et al.* Genomic Evidence Establishes Anatolia as the Source of the European Neolithic Gene Pool. *Curr. Biol.* **26**, 270–275 (2016).
52. Gallego Llorente, M. *et al.* Ancient Ethiopian genome reveals extensive Eurasian

admixture in Eastern Africa. *Science* **350,** 820–822 (2015).

53. Fu, Q. *et al.* The genetic history of Ice Age Europe. *Nature* **534,** 200–205 (2016).
54. Kilinc, G. M. *et al.* The Demographic Development of the First Farmers in Anatolia. *Curr. Biol.* **26,** 1–8 (2016).
55. Gallego-Llorente, M. *et al.* The genetics of an early Neolithic pastoralist from the Zagros, Iran. *Sci. Rep.* **6,** 4–10 (2016).
56. Olalde, I. *et al.* Derived immune and ancestral pigmentation alleles in a 7,000-year-old Mesolithic European. *Nature* **507,** 225–8 (2014).
57. Hofmanová, Z. *et al.* Early farmers from across Europe directly descended from Neolithic Aegeans. *Proc. Natl. Acad. Sci. U. S. A.* **113,** 6886–6891 (2016).
58. Patterson, N., Price, A. L. & Reich, D. Population structure and eigenanalysis. *PLoS Genet.* **2,** e190 (2006).
59. Purcell, S. *et al.* PLINK : A Tool Set for Whole-Genome Association and Population-Based Linkage Analyses. *Am. J. Hum. Genet.* **81,** 559–575 (2007).
60. Busing, F. M. T. A., Meijer, E. & Van Der Leeden, R. Delete- m Jackknife for Unequal m. *Stat. Comput.* **9,** 3–8 (1999).
61. Rojo-Guerra, M. Á., Kunst, M., Garrido-Pena, R. & García-Martínez de Lagrán, I. Morán-Dauchez, G. Un desafío a la eternidad. Tumbas monumentales del Valle de Ambrona. *Memorias Arqueología en Castilla y León 14, Junta de Castilla y León, Valladolid* (2005).
62. Gamba, C. *et al.* Genome flux and stasis in a five millennium transect of European prehistory. *Nat. Commun.* **5,** 5257 (2014).

Methods

Ancient DNA analysis

We screened skeletal samples for DNA preservation in dedicated clean rooms. We extracted DNA[34–36] and prepared barcoded next generation sequencing libraries, the majority of which were treated with uracil-DNA glycosylase to greatly reduce the damage (except at the terminal nucleotide) that is characteristic of ancient DNA[37,38] (Supplementary Information, section 4). We initially enriched libraries for sequences overlapping the mitochondrial genome[39] and ~3000 nuclear SNPs using synthesized baits (CustomArray Inc.) that we PCR amplified. We sequenced the enriched material on an Illumina NextSeq instrument with 2x76 cycles, and 2x7 cycles to read out the two indices[40]. We merged read pairs with the expected barcodes that overlapped by at least 15 bases, mapped the merged sequences to hg19 and to the reconstructed mitochondrial DNA consensus sequence[41] using the *samse* command in bwa (v0.6.1)[42], and removed duplicated sequences. We evaluated DNA authenticity by estimating the rate of mismatching to the consensus mitochondrial sequence[43], and also requiring that the rate of damage at the terminal nucleotide was at least 3% for UDG-treated libraries[43] and 10% for non-UDG-treated libraries[44].

For libraries that were promising after screening, we enriched in two consecutive rounds for sequences overlapping 1,233,013 SNPs ('1240k SNP capture')[2,10] and sequenced 2x76 cycles and 2x7 cycles on an Illumina NextSeq500 instrument. We processed the data bioinformatically as for the mitochondrial capture data, this time mapping only to the human reference genome *hg19* and merging the data from different libraries of the same individual. We further evaluated authenticity by studying the ratio of X-to-Y chromosome reads and estimating X-chromosome contamination in males based on the rate of heterozygosity[45]. Samples with evidence of contamination were either filtered out or restricted to sequences with terminal cytosine deamination to remove sequences that derived from modern contaminants. Finally, we filtered out from our genome-wide analysis dataset samples with fewer than 10,000 targeted SNPs covered at least once and samples that were first-degree relatives of others in the dataset (keeping the sample with the larger number of covered SNPs) (Supplementary Table 1).

Mitochondrial haplogroup determination

We used the mitochondrial capture bam files to determine the mitochondrial haplogroup of each sample with new data, restricting to sequences with MAPQ≥30 and base quality ≥30. First, we constructed a consensus sequence with samtools and bcftools[46], using a majority rule and requiring a minimum coverage of 2. We called haplogroups with HaploGrep2[47] based on phylotree[48] (mtDNA tree Build 17 (18 Feb 2016)). Mutational differences compared to the revised Cambridge Reference Sequence (rCRS) and corresponding haplogroups can be viewed in Supplementary Table 2.

Y-chromosome analysis

We determined Y-chromosome haplogroups for both new and published samples (Supplementary Information, section 5). We made use of the sequences mapping to 1240k Y-chromosome targets, restricting to sequences with mapping quality ≥30 and bases with quality ≥30. We called haplogroups by determining the most derived mutation for each sample, using the nomenclature of the International Society of Genetic Genealogy (http://www.isogg.org) version 11.110 (21 April 2016). Haplogroups and their supporting derived mutations can be viewed in Supplementary Table 3.

Merging newly generated data with published data

We assembled two datasets for genome-wide analyses:

-*HO* includes 2,572 present-day individuals from worldwide populations genotyped on the Human Origins Array[11,12,49] and 683 ancient individuals. The ancient set includes 211 Beaker Complex individuals (195 newly reported, 7 with shotgun data[3] for which we generated 1240k capture data and 9 previously published[3,4]), 68 newly reported individuals from relevant ancient populations and 298 previously published[12,18,19,21–23,50–57] individuals (Supplementary Table 1). We kept 591,642 autosomal SNPs after intersecting autosomal SNPs in the 1240k capture with the analysis set of 594,924 SNPs from Lazaridis et al.[11].

-*HOIll* includes the same set of ancient samples and 300 present-day individuals from 142 populations sequenced to high coverage as part of the Simons Genome Diversity Project[13]. For this dataset, we used 1,054,671 autosomal SNPs, excluding SNPs of the 1240k array located on sex chromosomes or with known functional effects.

For each individual, we represented the allele at each SNP by randomly sampling one sequence, discarding the first and the last two nucleotides of each sequence.

Principal component analysis

We carried out principal component analysis (PCA) on the *HO* dataset using the *smartpca* program in EIGENSOFT[58]. We computed principal components on 990 present-day West Eurasians and projected ancient individuals using lsqproject: YES and shrinkmode: YES.

ADMIXTURE analysis

We performed model-based clustering analysis using ADMIXTURE[17] on the *HO* reference dataset, including 2,572 present-day individuals from worldwide populations and the ancient individuals. First, we carried out LD-pruning on the dataset using PLINK[59] with the flag --indep-pairwise 200 25 0.4, leaving 306,393 SNPs. We ran ADMIXTURE with the cross validation (--cv) flag specifying from K=2 to K=20 clusters, with 20 replicates for each value of K and keeping for each value of K the replicate with highest log likelihood. In Extended Data Fig. 3b we show the cluster assignments at K=8 of newly reported individuals and other relevant ancient samples for comparison. We chose this value of K as it was the lowest one for which components of ancestry related both to Iranian Neolithic farmers and European Mesolithic hunter-gatherers were maximized.

f-statistics

We computed *f*-statistics on the *HOIll* dataset using ADMIXTOOLS[49] with default parameters (Supplementary Information, section 6). We used *qpDstat* with f4mode:Yes for f_4-statistics and *qp3Pop* for outgroup *f*3-statistics. We computed standard errors using a weighted block jackknife[60] over 5 Mb blocks.

Inference of mixture proportions

We estimated ancestry proportions on the *HOIll* dataset using *qpAdm*[2] and a basic set of 9 *Outgroups*: Mota, Ust_Ishim, MA1, Villabruna, Mbuti, Papuan, Onge, Han, Karitiana. For some analyses (Supplementary Information, section 8) we added additional outgroups to this basic set.

Admixture graph modelling

We modelled the relationships between populations in an Admixture Graph framework with the software *qpGraph* in ADMIXTOOLS[49], using the *HOIll* dataset and Mbuti as an outgroup (Supplementary Information, section 7).

Allele frequency estimation from read counts

We used allele counts at each SNP to perform maximum likelihood estimation of allele frequencies in ancient populations as in ref.[4]. In Extended Data Fig. 7, we show derived allele frequency estimates at three SNPs of functional importance for different ancient populations.

Data availability

All 1240k and mitochondrial capture sequencing data are available from the European Nucleotide Archive, accession number XXXXXXXX [to be made available on publication]. The genotype dataset we analysed is available from the Reich Lab website at [to be made available on publication].

Acknowledgements

We thank D. Anthony, J. Koch, I. Mathieson and C. Renfrew for comments and critiques. We thank A. C. Sousa for providing geographical information on a Portuguese sample. We thank A. Martín Cólliga from Generalitat de Catalunya and L. Loe for help in contacting archaeologists. We thank the Museo Arqueológico Regional de la Comunidad de Madrid for kindly allowing access to samples from Camino de las Yeseras. We thank C. Roth for sampling and sample preparation. We thank E. Carmona Ballesteros and M. Kunst for in sampling in Portugal and Spain. We thank A. Cooper for support from the Australian Centre for Ancient DNA. We thank the Hunterian Museum, University of Glasgow, for allowing access to samples from sites in Scotland, and particularly to Dr. S.-A. Coupar for help in accessing material. We thank the Museu Municipal de Torres Vedras for allowing the study and sampling of Cova da Moura collection. We thank the Bristol Radiocarbon Accelerator Mass Spectrometry Facility (BRAMS), Department of Archaeology and Anthropology, University of Bristol. We are grateful to the Orkney Museum for allowing access to samples from Orkney, and particularly to G. Drinkall for facilitating this work. We thank the Great North Museum: Hancock, the Society of Antiquaries of Newcastle upon Tyne, and Sunderland Museum for sharing samples, and M. Giesen for assisting with selection of those samples. We are grateful to E. Willerslev for sharing several dozen samples that were analyzed in this study and for supporting several co-authors at the Centre for GeoGenetics at the University of Copenhagen who worked on this project. We are grateful for institutional support (grant RVO:67985912) from the Institute of Archaeology, Czech Academy of Sciences. This work was supported by Momentum Mobility Research Group of the Hungarian Academy of Sciences. This work was supported by the Wellcome Trust [100713/Z/12/Z]. D.F. was supported by an Irish Research Council grant GOIPG/2013/36. P.W.S., J.K. and A.M. were supported by the Heidelberg Academy of Sciences (WIN project 'Times of Upheaval'). K.K. was supported by The Swedish Foundation for Humanities and Social Sciences under Project Grant M16-0455:1. M.Fu. was supported by the National Science Centre, Poland (the Sonata-Bis 3 project no DEC-2013/10/E/HS3/00141). C.L.-F. was supported by a grant from FEDER and MINECO (BFU2015-64699-P) of Spain. C.L., P.R. and C.B. were supported by a grant from MINECO (HAR2016-77600-P), Spanish Government. D.R. was supported by US National Science Foundation HOMINID grant BCS-1032255, US National Institutes of Health grant GM100233, and is an investigator of the Howard Hughes

Medical Institute. Radiocarbon work at Penn State was supported by the NSF Archaeometry (BCS-1460369, D.J.K.) and Archaeology (BCS-1725067, D.J.K and T. H.) programs.

Author Contributions

S.B., M.E.A, N.R., A.Sz.-N., A.M., N.B., M.F., E.H., M.M., J.O., K.S., O.C., D.K., F.C., R.P., J.K., W.H., I.B. and D.R. performed or supervised wet laboratory work. G.T.C. and D.J.K. undertook the radiocarbon dating of a large fraction of samples. I.A., K.K., A.B., K.W.A., A.A.F., E.B., M.B.-B., D.B., C.B., J.V.M., R.M., C.Bo., L.B., T.A., L.Bü., S.C., L.C.N., O.E.C., G.C., B.C., A.D., K.E.D., N.D., M.E., C.E., M.K., J.F.F., H.F., C.F., M.G., R.G.P., M.H.-U., E.Had., G.H., N.J., T.K., K.M., S.P., P.L., O.L., A.L., C.H.M., V.G.O., A.B.R., J.L.M., T.M., J.I.M, K.Mc., M.B.G., A.Mo., G.K., V.K., A.C., R.Pa., A.E., K.Kö., T.H., T.S., J.D., Z.B., M.H., P.V., M.D., F.B., R.F.F., A. H.-C., S.T., E.C., L.L., A.V., A.Z., C.W., G.D., E.G.-D., B.N., M.B., M.Lu., R.Mo., J.De., M.Be., G.B., M.Fu., A.H., M.Ma., A.R., S.L., I.S., K.T.L., J.L.C., C.L., M.P.P., P.W., T.D.P., P.P., P.-J.R., P.R., R.R., M.A.R.G., A.S., J.S., A.M.S., V.S., L.V., J.Z., D.C., T.Hi., V.H., A.Sh., K.-G.S., P.W.S., R.P., J.K., W.H., I.B., C.L.-F. and D.R. assembled archaeological material. I.O., S.M., T.B., A.M., E.A., M.L., I.L., N.P., Y.D., Z.F., D.F., D.J.K., P.d.K., T.K.H., M.G.T. and D.R. analysed or supervised analysis of data. I.O., C.L.-F. and D.R. wrote the manuscript with input from all co-authors.

Supplementary Tables

Supplementary Table 1. Ancient individuals included in this study.

Supplementary Table 2. Mitochondrial haplogroup calls for individuals with newly reported data.

Supplementary Table 3. Y-chromosome calls for males with newly reported data.

Supplementary Table 4. Radiocarbon database.

Extended Data Figure 1. **Beaker complex artefacts**. **a**, ‘All-Over-Cord’ Beaker from Bathgate, West Lothian, Scotland. Photo: National Museums Scotland. **b**, Beaker Complex grave goods from La Sima III barrow, Soria, Spain[61]. The set includes Beaker pots of the so-called ‘Maritime style’. Photo: Alejandro Plaza, Museo Numantino.

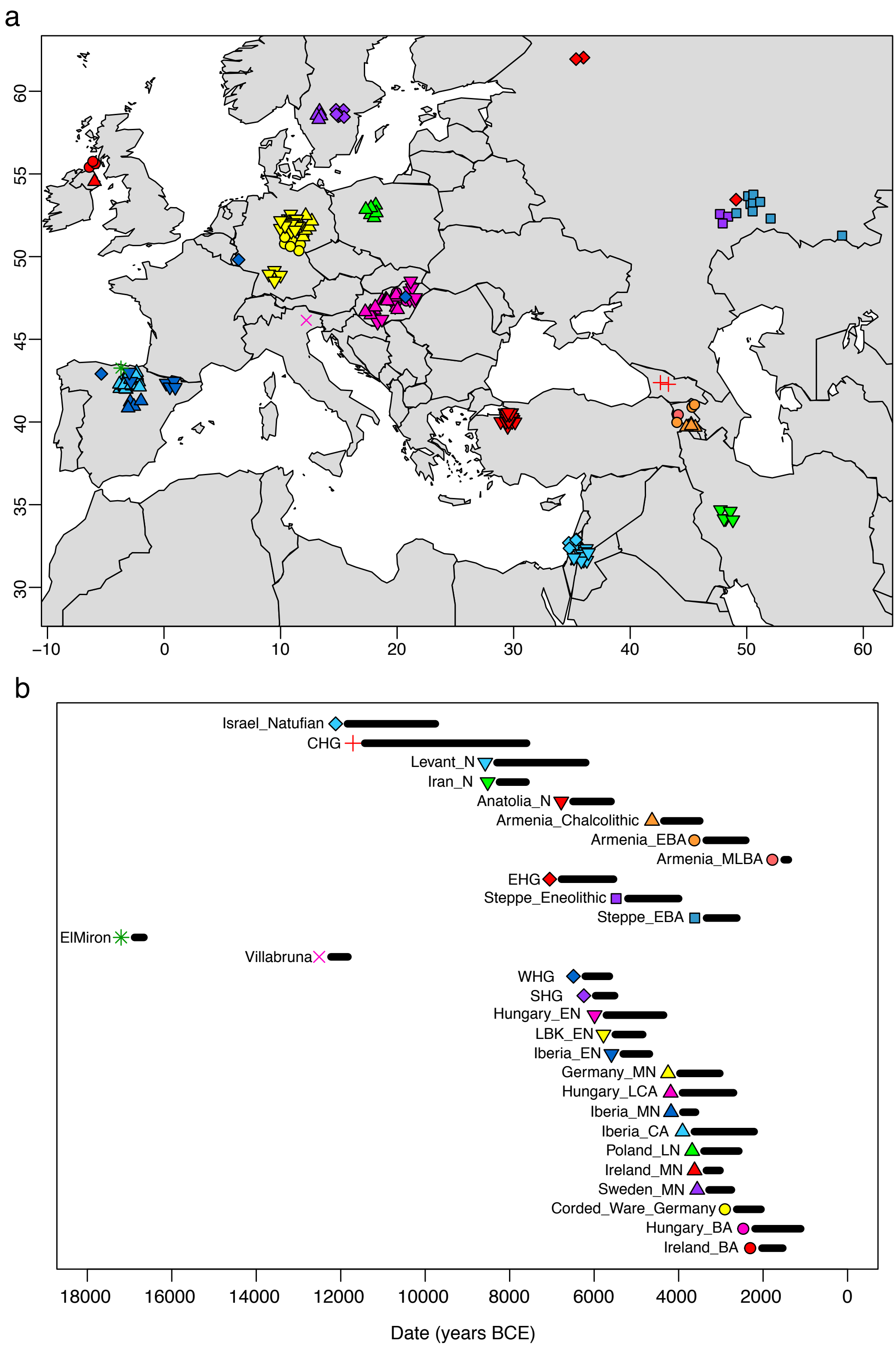

Extended Data Figure 2. Ancient individuals with previously published genome-wide data used in this study. **a,** Sampling locations. **b,** Time ranges. W/E/S/CHG, Western/Eastern/Scandinavian/Caucasus hunter-gatherers; E, Early; M, Middle; L, Late; N, Neolithic; CA, Copper Age; BA, Bronze Age.

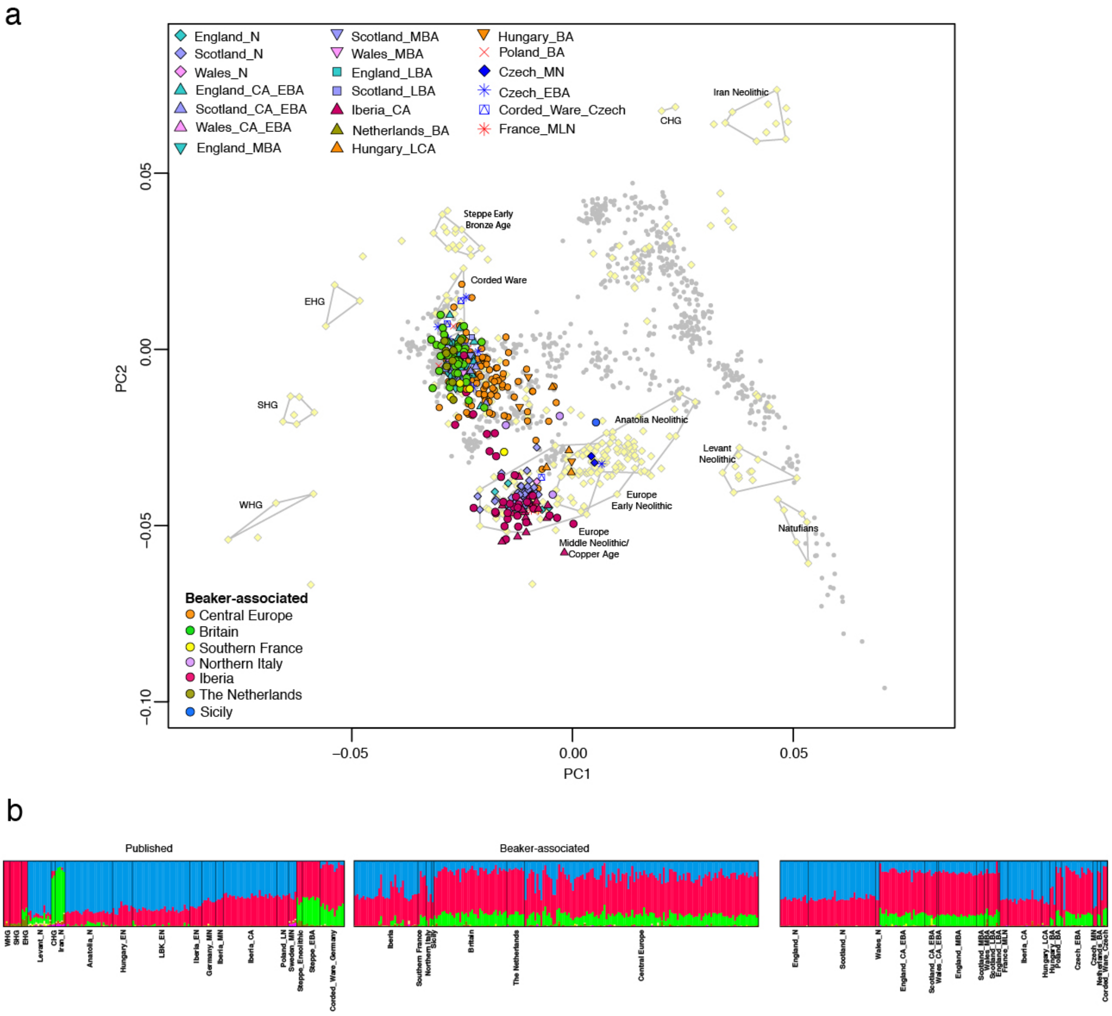

Extended Data Figure 3. Population structure. a, Principal component analysis of 990 present-day West Eurasian individuals (grey dots), with previously published (pale yellow) and new ancient samples projected onto the first two principal components. **b**, ADMIXTURE clustering analysis with k=8 showing ancient individuals. W/E/S/CHG, Western/Eastern/Scandinavian/Caucasus hunter-gatherers; E, Early; M, Middle; L, Late; N, Neolithic; CA, Copper Age; BA, Bronze Age.

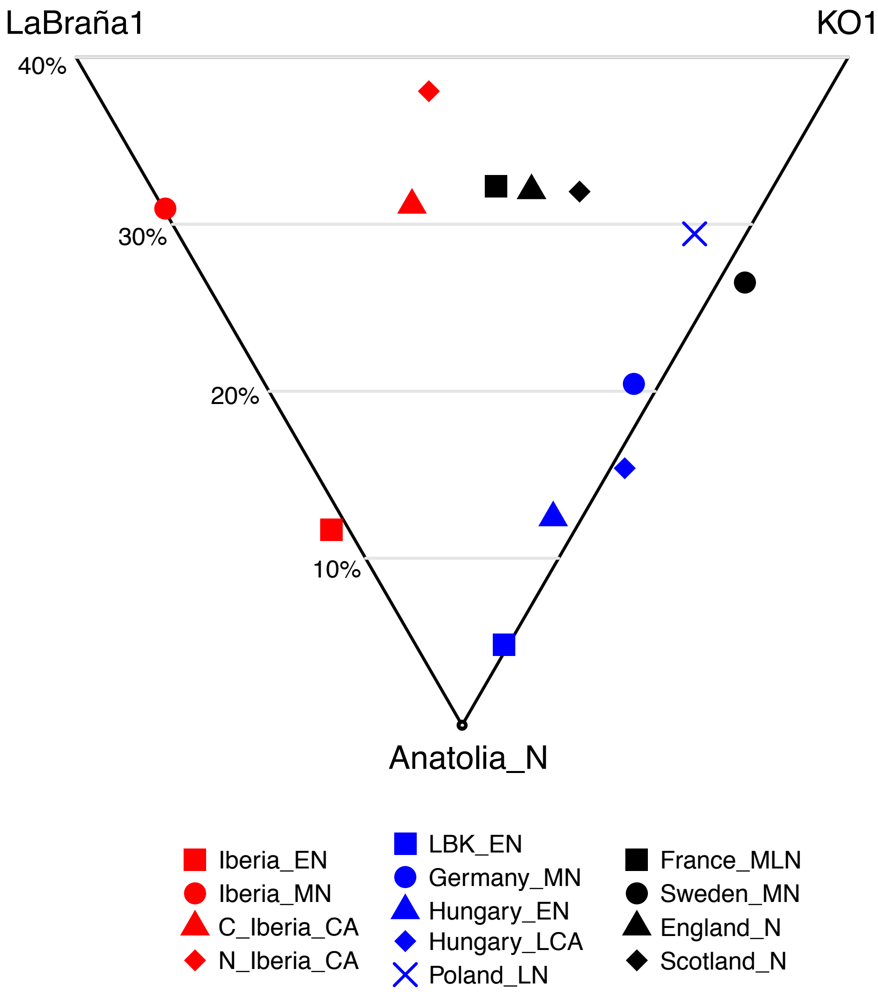

Extended Data Figure 4. Hunter-gatherer affinities in Neolithic/Copper Age Europe. Differential affinity to hunter-gatherer individuals (LaBraña1[56] from Spain and KO1[62] from Hungary) in European populations before the emergence of the Beaker Complex. See Supplementary Information, section 8 for mixture proportions and standard errors computed with *qpAdm*. E, Early; M, Middle; L, Late; N, Neolithic; CA, Copper Age; BA, Bronze Age; N_Iberia, Northern Iberia; C_Iberia, Central Iberia.

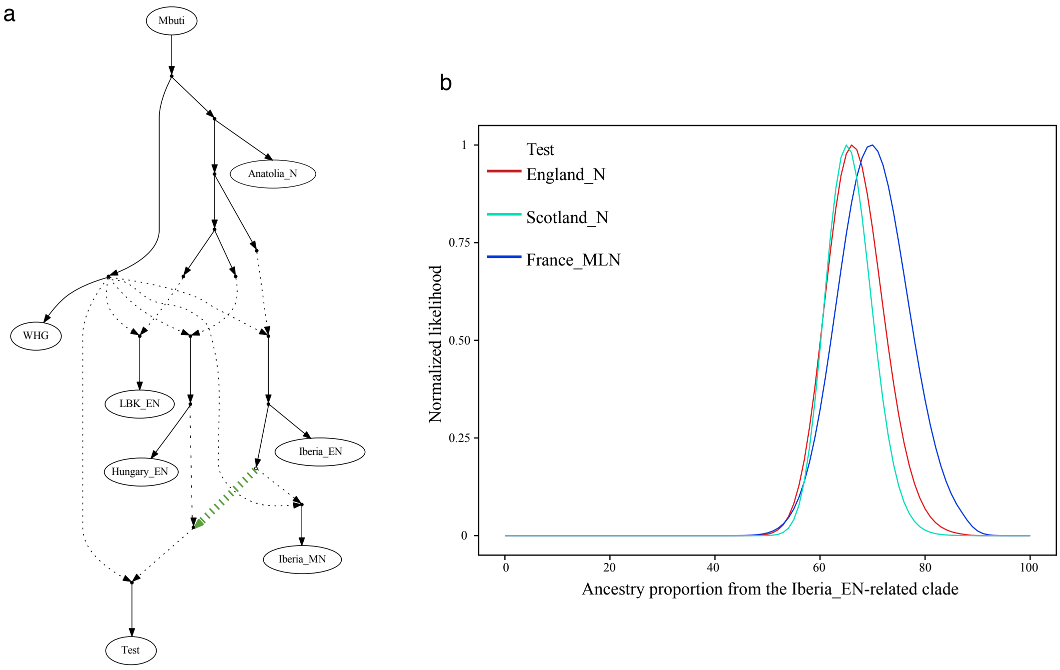

Extended Data Figure 5. **Modelling the relationships between Neolithic populations**. **a,** Admixture graph fitting a *Test* population as a mixture of sources related to both Iberia_EN and Hungary_EN. **b,** Likelihood distribution for models with different proportions of the source related to Iberia_EN (green admixture edge in (a)) when *Test* is England_N, Scotland_N or France_MLN. E, Early; M, Middle; L, Late; N, Neolithic.

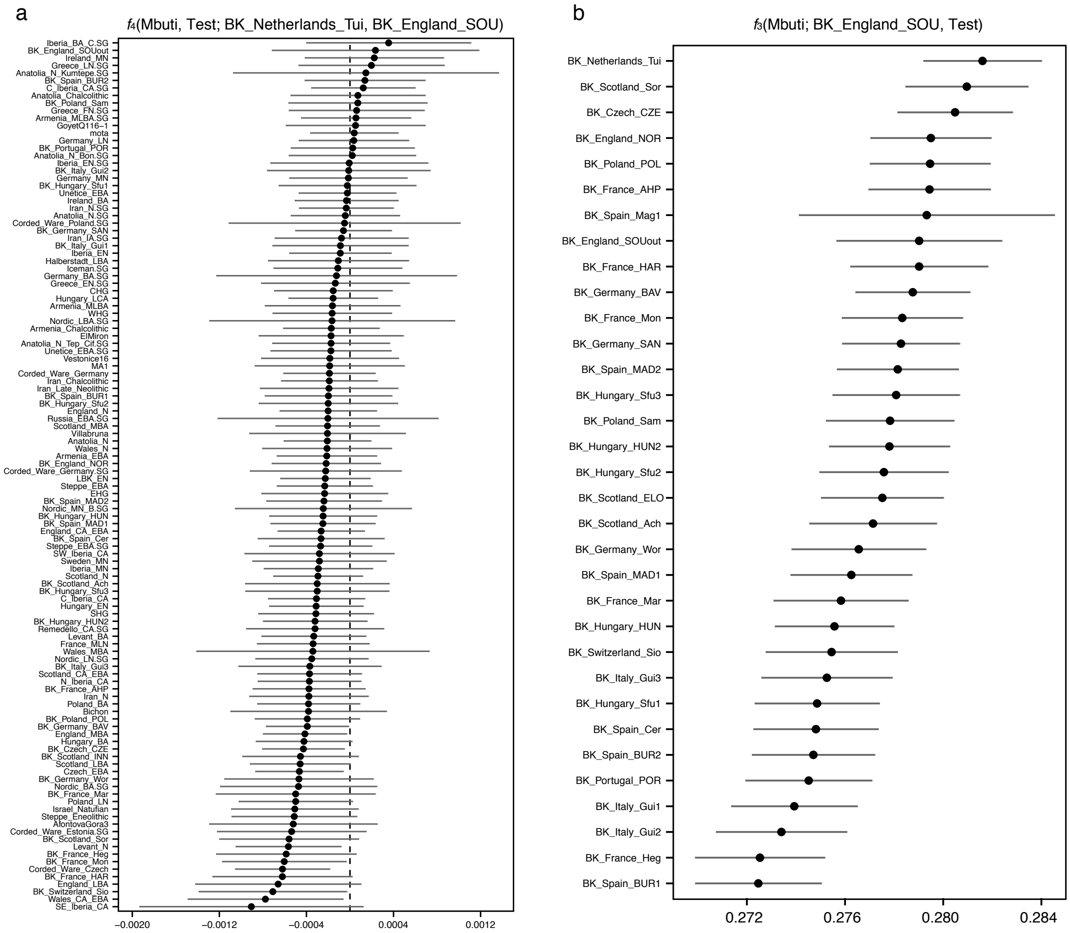

Extended Data Figure 6. **Genetic affinity between Beaker Complex-associated individuals from southern England and the Netherlands**. **a**, *f*-statistics of the form f_4(Mbuti, Test; BK_Netherlands_Tui, BK_England_SOU). Negative values indicate that Test is closer to BK_Netherlands_Tui than to BK_England_SOU, and the opposite for positive values. Error bars represent ±3 standard errors. **b**, Outgroup-f_3 statistics of the form f_3(Mbuti; BK_England_SOU, Test) measuring shared genetic drift between BK_England_SOU and other Beaker Complex-associated groups. Error bars represent ±1 standard errors. BK_Netherlands_Tui, Beaker-associated individuals from De Tuithoorn, Oostwoud, the Netherlands; BK_England_SOU, Beaker-associated individuals from southern England. See Supplementary Table 1 for individuals associated to each population label.

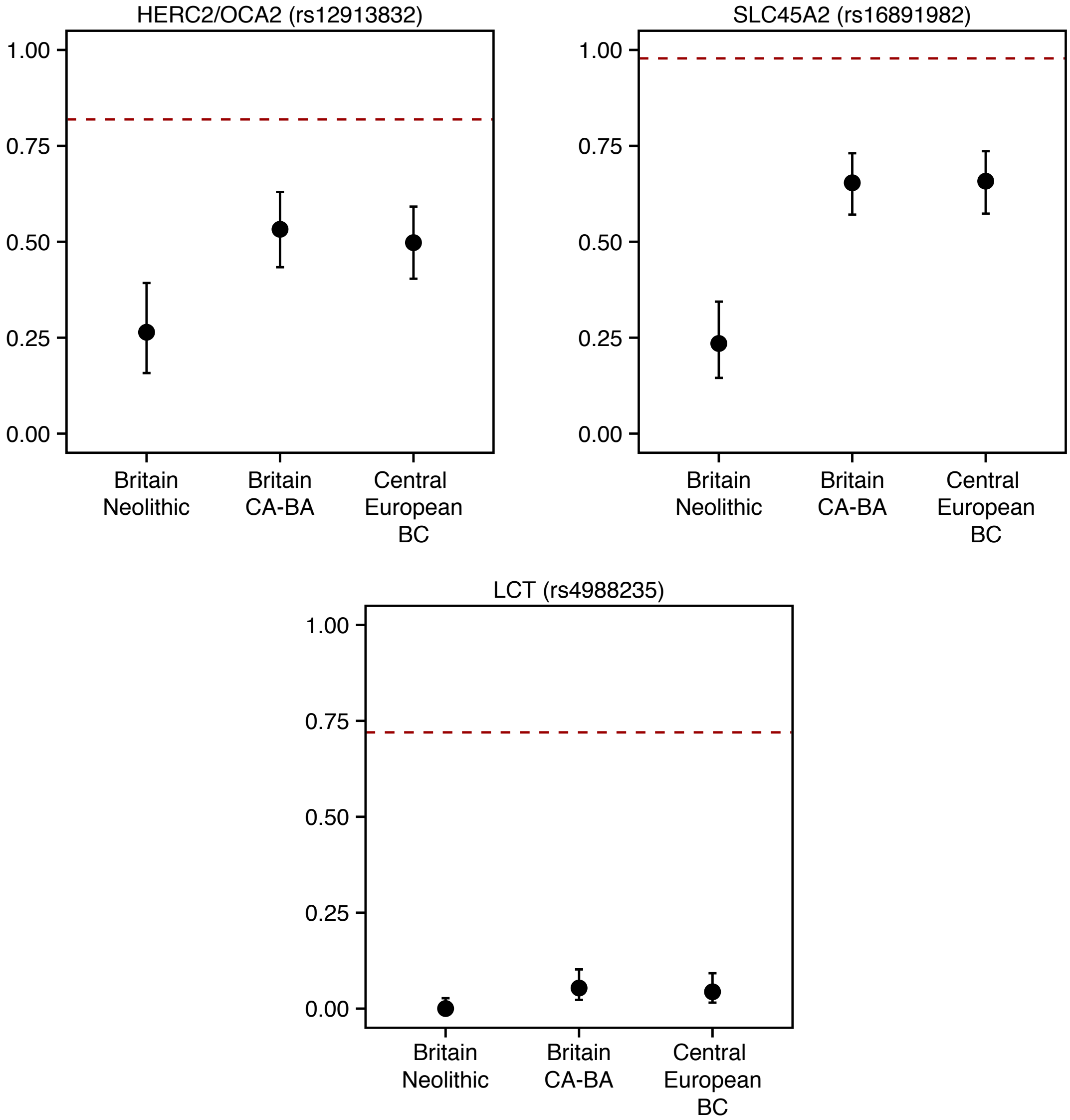

Extended Data Figure 7. Derived allele frequencies at three SNPs of functional importance. Error bars represent 1.9-log-likelihood support interval. The red dashed lines show allele frequencies in the 1000 Genomes GBR population (present-day people from Great Britain). BC, Beaker Complex; CA, Copper Age; BA, Bronze Age.

Extended Data Table 1. Sites with new genome-wide data reported in this study.

Site	N	Approx. date range (BCE)	Country
Brandysek	12	2900–2200	Czech Republic
Kněževes	2	2500–1900	Czech Republic
Lochenice	1	2500–1900	Czech Republic
Lovosice II	1	2500–1900	Czech Republic
Moravská Nová Ves	4	2300–1900	Czech Republic
Prague 5 - Malá Ohrada	14	2500–2200	Czech Republic
Prague 5, Jinonice	14	2200–1700	Czech Republic
Prague 8, Kobylisy, Ke Stírce Street	12	2500–1900	Czech Republic
Radovesice	13	2500–2200	Czech Republic
Velké Přílepy	3	2500–1900	Czech Republic
Clos de Roque, Saint Maximin-la-Sainte-Baume	3	4700–4500	France
Collet Redon, La Couronne-Martigues	1	3500–3100	France
Hégenheim Necropole, Haut-Rhin	1	2800–2500	France
La Fare, Forcalquier	1	2500–2200	France
Marlens, Sur les Barmes, Haute-Savoie	1	2500–2100	France
Mondelange, PAC de la Sente, Moselle	2	2400–1900	France
Rouffach, Haut-Rhin	1	2300–2100	France
Sierentz, Les Villas d'Aurele, Haut-Rhin	2	2600–2300	France
Villard, Lauzet-Ubaye	2	2200–1900	France
Alburg-Lerchenhaid, Spedition Häring, Bavaria	13	2500–2100	Germany
Augsburg Sportgelände, Augsburg, Bavaria	6	2500–2000	Germany
Hugo-Eckener-Straße, Augsburg, Bavaria	3	2500–2000	Germany
Irlbach, County of Straubing-Bogen, Bavaria	17	2500–2000	Germany
Künzing-Bruck, Lkr. Deggendorf, Bavaria	3	2500–2000	Germany
Landau an der Isar, Bavaria	5	2500–2000	Germany
Manching-Oberstimm, Bavaria	2	2500–2000	Germany
Osterhofen-Altenmarkt, Bavaria	4	2600–2000	Germany
Unterer Talweg 58-62, Augsburg, Bavaria	2	2500–2200	Germany
Unterer Talweg 85, Augsburg, Bavaria	1	2400–2100	Germany
Weichering, Bavaria	4	2500–2000	Germany
Worms-Herrnsheim, Rhineland-Palatinate	1	2500–2000	Germany
Aberdour Road, Dunfermline, Fife, Scotland	1	2000–1800	Great Britain
Abingdon Spring Road cemetery, Oxfordshire, England	1	2500–2200	Great Britain
Achavanich, Wick, Highland, Scotland	1	2500–2100	Great Britain
Amesbury Down, Wiltshire, England	13	2500–1300	Great Britain
Banbury Lane, Northamptonshire, England	3	3400–3100	Great Britain
Barrow Hills, Radley, Oxfordshire, England	1	2300–1800	Great Britain
Barton Stacey, Hampshire, England	1	2200–2000	Great Britain
Baston and Langtoft, South Lincolnshire, England	2	1700–1600	Great Britain
Biddenham Loop, Bedfordshire, England	9	1600–1300	Great Britain
Boatbridge Quarry, Thankerton, Scotland	1	2400–2100	Great Britain
Boscombe Airfield, Wiltshire, England	1	1800–1600	Great Britain
Canada Farm, Sixpenny Handley, Dorset, England	2	2500–2300	Great Britain
Carsington Pasture Cave, Derbyshire, England	2	3700–2000	Great Britain
Central Flying School, Upavon, Wiltshire, England	1	2500–1800	Great Britain
Cissbury Flint Mine, Worthing, West Sussex, England	1	3600–3400	Great Britain
Clachaig, Arran, North Ayrshire, Scotland	1	3500–3400	Great Britain
Clay Farm, Cambridgeshire, England	2	1400–1300	Great Britain
Covesea Cave 2, Moray, Scotland	3	2100–800	Great Britain
Covesea Caves, Moray, Scotland	2	1000–800	Great Britain
Culver Hole Cave, Port Eynon, West Glamorgan, Wales	1	1600–800	Great Britain
Dairy Farm, Willington, England	1	2300–1900	Great Britain
Distillery Cave, Oban, Argyll and Bute, Scotland	3	3800–3400	Great Britain
Ditchling Road, Brighton, Sussex, England	1	2500–1900	Great Britain
Doune, Perth and Kinross, Scotland	1	1800–1600	Great Britain
Dryburn Bridge, East Lothian, Scotland	2	2300–1900	Great Britain
Eton Rowing Course, Buckinghamshire, England	2	3600–2900	Great Britain
Eweford Cottages, East Lothian, Scotland	1	2100–1900	Great Britain
Flying School, Netheravon, Wiltshire, England	2	2500–1800	Great Britain
Fussell's Lodge, Salisbury, Wiltshire, England	2	3800–3600	Great Britain
Lesser Kelco Cave, North Yorkshire, England	1	3700–3500	Great Britain
Great Orme Mines, Llandudno, North Wales	1	1700–1600	Great Britain
Hasting Hill, Sunderland, Tyne and Wear, England	2	2500–1800	Great Britain
Hexham Golf Course, Northumberland, England	1	2000–1800	Great Britain
Holm of Papa Westray North, Orkney, Scotland	4	3500–3100	Great Britain
Isbister, Orkney, Scotland	10	3300–2300	Great Britain
Leith, Merrilees Close, City of Edinburgh, Scotland	2	1600–1500	Great Britain

Longniddry, Evergreen House, East Lothian, Scotland	3	1500–1300	Great Britain
Longniddry, Grainfoot, East Lothian, Scotland	1	1300–1000	Great Britain
Low Hauxley, Northumberland, England	2	2100–1600	Great Britain
Macarthur Cave, Oban, Argyll and Bute, Scotland	1	4000–3800	Great Britain
Melton Quarry, East Riding of Yorkshire, England	1	1900–1700	Great Britain
Neale's Cave, Paington, Devon, England	1	2000–1600	Great Britain
North Face Cave, Llandudno, North Wales	1	1400–1200	Great Britain
Nr. Ablington, Figheldean, England	1	2500–1800	Great Britain
Nr. Millbarrow, Wiltshire, England	1	3600–3400	Great Britain
Over Narrows, Needingworth Quarry, England	5	2200–1300	Great Britain
Pabay Mor, Lewis, Western Isles, Scotland	1	1400–1300	Great Britain
Point of Cott, Orkney, Scotland	2	3700–3100	Great Britain
Porton Down, Wiltshire, England	2	2500–1900	Great Britain
Quoyness, Orkney, Scotland	1	3100–2900	Great Britain
Raschoille Cave, Oban, Argyll and Bute, Scotland	9	4000–2900	Great Britain
Raven Scar Cave, Ingleton, North Yorkshire, England	1	1100–900	Great Britain
Reaverhill, Barrasford, Northumberland, England	1	2100–2000	Great Britain
Rhos Ddigre, Llanarmon-yn-Iâl, Denbighshire, Wales	1	3100–2900	Great Britain
River Thames, Mortlake/Syon Reach, London, England	2	2500–1700	Great Britain
Sorisdale, Coll, Argyll and Bute, Scotland	1	2500–2100	Great Britain
Staxton Beacon, Staxton,England	1	2400–1600	Great Britain
Stenchme, Lop Ness, Orkney, Scotland	1	2000–1500	Great Britain
Summerhill,Blaydon, Tyne and Wear, England	1	1900–1700	Great Britain
Thanet, Kent, England	4	2100–1700	Great Britain
Thurston Mains, Innerwick, East Lothian, Scotland	1	2300–2000	Great Britain
Tinkinswood, Cardiff, Glamorgan, Wales	1	3800–3600	Great Britain
Totty Pot, Cheddar, Somerset, England	1	2800–2500	Great Britain
Trumpington Meadows, Cambridge, England	2	2200–2000	Great Britain
Tulach an t'Sionnach, Highland, Scotland	1	3700–3500	Great Britain
Tulloch of Assery A, Highland, Scotland	1	3700–3400	Great Britain
Tulloch of Assery B, Highland, Scotland	1	3800–3600	Great Britain
Turners Yard, Fordham, Cambridgeshire, England	1	1700–1500	Great Britain
Unstan, Orkney, Scotland	1	3400–3100	Great Britain
Upper Swell, Chipping Norton, Gloucestershire, England	1	4000–3300	Great Britain
Waterhall Farm, Chippenham, Cambridgeshire, England	1	2000–1700	Great Britain
West Deeping, Lincolnshire, England	1	2300–2000	Great Britain
Whitehawk, Brighton, Sussex, England	1	3700–3400	Great Britain
Wick Barrow, Stogursey, Somerset, England	1	2400–2000	Great Britain
Wilsford Down, Wilsford-cum-Lake, Wiltshire, England	2	2400–2000	Great Britain
Windmill Fields, North Yorkshire, England	4	2300–2000	Great Britain
Yarnton, Oxfordshire, England	4	2500–1900	Great Britain
Budakalász, Csajerszke (M0 Site 12)	2	2600–2200	Hungary
Budapest-Békásmegyer	3	2500–2100	Hungary
Mezőcsát-Hörcsögös	4	3400–3000	Hungary
Szigetszentmiklós-Üdülősor	4	2500–2200	Hungary
Szigetszentmiklós, Felső Ürge-hegyi dűlő	6	2500–2200	Hungary
Pergole 2, Partanna, Sicily	3	2500–1900	Italy
Via Guidorossi, Parma, Emilia Romagna	3	2200–1900	Italy
Dzielnica	1	2300–2000	Poland
Iwiny	1	2300–2000	Poland
Jordanów Śląski	1	2300–2200	Poland
Kornice	4	2500–2100	Poland
Racibórz-Stara Wieś	1	2300–2000	Poland
Samborzec	3	2500–2100	Poland
Strachów	1	2000–1800	Poland
Żerniki Wielkie	1	2300–2100	Poland
Bolores, Estremadura	1	2800–2600	Portugal
Cova da Moura, Torres Vedras	1	2300–2100	Portugal
Galeria da Cisterna, Almonda	2	2500–2200	Portugal
Verdelha dos Ruivos, District of Lisbon	3	2700–2300	Portugal
Arroyal I, Burgos	5	2600–2200	Spain
Camino de las Yeseras, Madrid	14	2800–1700	Spain
Camino del Molino, Caravaca, Murcia	4	2900–2100	Spain
Humanejos, Madrid	11	2900–2000	Spain
La Magdalena, Madrid	3	2500–2000	Spain
Paris Street, Cerdanyola, Barcelona	10	2900–2300	Spain
Virgazal, Tablada de Rudrón, Burgos	1	2300–2000	Spain
Sion-Petit-Chasseur, Dolmen XI	3	2500–2000	Switzerland
De Tuithoorn, Oostwoud, Noord-Holland	11	2600–1600	The Netherlands

Extended Data Table 2. 111 newly reported radiocarbon dates

Sample	Date	Location	Country
I5024	2278–2032 calBCE (3740±35 BP, Poz-84460)	Kněževes	Czech Republic
I4946	2296–2146 calBCE (3805±20 BP, PSUAMS-2801)	Prague 5, Jinonice, Butovická Street	Czech Republic
I4895	2273–2047 calBCE (3750±20 BP, PSUAMS-2852)	Prague 5, Jinonice, Butovická Street	Czech Republic
I4896	2288–2142 calBCE (3785±20 BP, PSUAMS-2853)	Prague 5, Jinonice, Butovická Street	Czech Republic
I4884	1882–1745 calBCE (3480±20 BP, PSUAMS-2842)	Prague 8, Kobylisy, Ke Stírce Street	Czech Republic
I4885	2289–2143 calBCE (3790±20 BP, PSUAMS-2843)	Prague 8, Kobylisy, Ke Stírce Street	Czech Republic
I4886	2205–2042 calBCE (3740±20 BP, PSUAMS-2844)	Prague 8, Kobylisy, Ke Stírce Street	Czech Republic
I4887	2201–2039 calBCE (3730±20 BP, PSUAMS-2845)	Prague 8, Kobylisy, Ke Stírce Street	Czech Republic
I4888	2190–2029 calBCE (3700±20 BP, PSUAMS-2846)	Prague 8, Kobylisy, Ke Stírce Street	Czech Republic
I4889	2281–2062 calBCE (3765±20 BP, PSUAMS-2847)	Prague 8, Kobylisy, Ke Stírce Street	Czech Republic
I4891	2281–2062 calBCE (3765±20 BP, PSUAMS-2848)	Prague 8, Kobylisy, Ke Stírce Street	Czech Republic
I4892	1881–1701 calBCE (3475±20 BP, PSUAMS-2849)	Prague 8, Kobylisy, Ke Stírce Street	Czech Republic
I4893	4449–4348 calBCE (5550±20 BP, PSUAMS-2850)	Prague 8, Kobylisy, Ke Stírce Street	Czech Republic
I4894	4488–4368 calBCE (5610±20 BP, PSUAMS-2851)	Prague 8, Kobylisy, Ke Stírce Street	Czech Republic
I4945	2291–2144 calBCE (3795±20 BP, PSUAMS-2854)	Prague 8, Kobylisy, Ke Stírce Street	Czech Republic
I4305	4825–4616 calBCE (5860±35 BP, PSUAMS-2225)	Clos de Roque, Saint Maximin-la-Sainte-Baume	France
I4304	4787–4589 calBCE (5830±35 BP, PSUAMS-2226)	Clos de Roque, Saint Maximin-la-Sainte-Baume	France
I4303	4778–4586 calBCE (5820±30 BP, PSUAMS-2260)	Clos de Roque, Saint Maximin-la-Sainte-Baume	France
I1392	2833–2475 calBCE (4047±29 BP, MAMS-25935)	Hégenheim Necropole, Haut-Rhin	France
I3875	2133–1946 calBCE (3655±25 BP, PSUAMS-1834)	Villard, Lauzet-Ubaye	France
I3874	2200–2035 calBCE (3725±25 BP, PSUAMS-1835)	Villard, Lauzet-Ubaye	France
I3593	2397–2145 calBCE (3817±26 BP, BRAMS-1215)	Alburg-Lerchenhaid, Spedition Häring, Bavaria	Germany
I3590	2335–2140 calBCE (3802±26 BP, BRAMS-1217)	Alburg-Lerchenhaid, Spedition Häring, Bavaria	Germany
I3592	2457–2203 calBCE (3844±33 BP, BRAMS-1218)	Alburg-Lerchenhaid, Spedition Häring, Bavaria	Germany
I5017	2460–2206 calBCE (3855±35 BP, Poz-84458)	Augsburg Sportgelände, Augsburg, Bavaria	Germany
I4250	2433–2149 calBCE (3825±26 BP, BRAMS-1219)	Irlbach, County of Straubing-Bogen, Bavaria	Germany
I5021	2571–2341 calBCE (3955±35 BP, Poz-84553)	Osterhofen-Altenmarkt, Bavaria	Germany
E09537_d	2471–2298 calBCE (3909±29 BP, MAMS-29074)	Unterer Talweg 58-62, Augsburg, Bavaria	Germany
E09538	2464–2210 calBCE (3870±30 BP, MAMS-29075)	Unterer Talweg 58-62, Augsburg, Bavaria	Germany
I5385	2455–2147 calBCE (3827±33 BP, SUERC-71005)	Achavanich, Wick, Highland, Scotland	Great Britain
I2457	2199–2030 calBCE (3717±28 BP, SUERC-69975)	Amesbury Down, Wiltshire, England	Great Britain
I2416	2455–2151 calBCE (3830±30 BP, Beta-432804)	Amesbury Down, Wiltshire, England	Great Britain
I2596	2273–2034 calBCE (3739±30 BP, NZA-32484)	Amesbury Down, Wiltshire, England	Great Britain
I2566	2204–2035 calBCE (3734±25 BP, NZA-32490)	Amesbury Down, Wiltshire, England	Great Britain
I2598	2135–1953 calBCE (3664±30 BP, NZA-32494)	Amesbury Down, Wiltshire, England	Great Britain
I2418	2455–2200 calBCE (3836±25 BP, NZA-32788)	Amesbury Down, Wiltshire, England	Great Britain
I2565	2457–2147 calBCE (3829±38 BP, OxA-13562)	Amesbury Down, Wiltshire, England	Great Britain
I2457	2467–2290 calBCE (3890±30 BP, SUERC-36210)	Amesbury Down, Wiltshire, England	Great Britain
I2460	2022–1827 calBCE (3575±27 BP, SUERC-53041)	Amesbury Down, Wiltshire, England	Great Britain
I2459	2455–2150 calBCE (3829±30 BP, SUERC-54823)	Amesbury Down, Wiltshire, England	Great Britain
I5373	2194–1980 calBCE (3694±25 BP, BRAMS-1230)	Carsington Pasture Cave, Brassington, Derbyshire, England	Great Britain
I2988	3516–3361 calBCE (4645±29 BP, SUERC-68711)	Clachaig, Arran, North Ayrshire, Scotland	Great Britain
I2860	969–815 calBCE (2738±29 BP, SUERC-68715)	Covesea Cave 2, Moray, Scotland	Great Britain
I2861	976–828 calBCE (2757±29 BP, SUERC-68716)	Covesea Cave 2, Moray, Scotland	Great Britain
I3132	2118–1887 calBCE (3614±33 BP, SUERC-69070)	Covesea Cave 2, Moray, Scotland	Great Britain
I3130	977–829 calBCE (2758±29 BP, SUERC-68713)	Covesea Caves, Moray, Scotland	Great Britain
I2859	910–809 calBCE (2714±29 BP, SUERC-68714)	Covesea Caves, Moray, Scotland	Great Britain
I2452	2198–1980 calBCE (3700±30 BP, Beta-444979)	Dairy Farm, Willington, England	Great Britain
I2452	2276–2029 calBCE (3735±35 BP, Poz-83405)	Dairy Farm, Willington, England	Great Britain
I2659	3761–3643 calBCE (4914±27 BP, SUERC-68702)	Distillery Cave, Oban, Argyll and Bute, Scotland	Great Britain
I2660	3513–3352 calBCE (4631±29 BP, SUERC-68703)	Distillery Cave, Oban, Argyll and Bute, Scotland	Great Britain
I2691	3700–3639 calBCE (4881±25 BP, SUERC-68704)	Distillery Cave, Oban, Argyll and Bute, Scotland	Great Britain
I6774	2287–2044 calBCE (3760±30 BP, SUERC-74755)	Ditchling Road, Brighton, Sussex, England	Great Britain
I2605	3631–3372 calBCE (4710±35 BP, Poz-83483)	Eton Rowing Course, Buckinghamshire, England	Great Britain
I1775	1730–1532 calBCE (3344±27 BP, OxA-14308)	Great Orme, Llandudno, North Wales	Great Britain
I2574	1414–1227 calBCE (3065±36 BP, SUERC-62072)	Great Orme, Llandudno, North Wales	Great Britain
I2612	2464–2208 calBCE (3865±35 BP, Poz-83492)	Hasting Hill, Sunderland, Tyne and Wear, England	Great Britain
I2609	2022–1771 calBCE (3560±40 BP, Poz-83423)	Hexham Golf Course, Northumberland, England	Great Britain
I2636	3519–3361 calBCE (4651±33 BP, SUERC-68640)	Holm of Papa Westray North, Orkney, Scotland	Great Britain
I2637	3629–3370 calBCE (4697±33 BP, SUERC-68641)	Holm of Papa Westray North, Orkney, Scotland	Great Britain
I2650	3638–3380 calBCE (4754±36 BP, SUERC-68642)	Holm of Papa Westray North, Orkney, Scotland	Great Britain

I2651	3360–3098 calBCE (4525±36 BP, SUERC-68643)	Holm of Papa Westray North, Orkney, Scotland	Great Britain
I2630	2580–2463 calBCE (3999±32 BP, SUERC-68632)	Isbister, Orkney, Scotland	Great Britain
I2932	2570–2347 calBCE (3962±29 BP, SUERC-68721)	Isbister, Orkney, Scotland	Great Britain
I2933	3010–2885 calBCE (4309±29 BP, SUERC-68722)	Isbister, Orkney, Scotland	Great Britain
I2935	3335–3011 calBCE (4451±29 BP, SUERC-68723)	Isbister, Orkney, Scotland	Great Britain
I3085	3338–3026 calBCE (4471±29 BP, SUERC-68724)	Isbister, Orkney, Scotland	Great Britain
I2978	3335–3023 calBCE (4464±29 BP, SUERC-68725)	Isbister, Orkney, Scotland	Great Britain
I2979	3333–2941 calBCE (4447±29 BP, SUERC-68726)	Isbister, Orkney, Scotland	Great Britain
I2934	3338–3022 calBCE (4466±33 BP, SUERC-69071)	Isbister, Orkney, Scotland	Great Britain
I2977	3008–2763 calBCE (4275±33 BP, SUERC-69072)	Isbister, Orkney, Scotland	Great Britain
I2657	3951–3780 calBCE (5052±30 BP, SUERC-68701)	Macarthur Cave, Oban, Argyll and Bute, Scotland	Great Britain
I5441	1938–1744 calBCE (3512±37 BP, OxA-16522)	Neale's Cave, Paington, Devon, England	Great Britain
I4949	3629–3376 calBCE (4715±20 BP, PSUAMS-2513)	Nr. Millbarrow, Winterbourne Monkton, Wiltshire, England	Great Britain
I2980	3360–3101 calBCE (4530±33 BP, SUERC-69073)	Point of Cott, Orkney, Scotland	Great Britain
I2796	3705–3535 calBCE (4856±33 BP, SUERC-69074)	Point of Cott, Orkney, Scotland	Great Britain
I2631	3097–2906 calBCE (4384±36 BP, SUERC-68633)	Quoyness, Orkney, Scotland	Great Britain
I3135	3640–3383 calBCE (4770±30 BP, PSUAMS-2068)	Raschoille Cave, Oban, Argyll and Bute, Scotland	Great Britain
I3136	3520–3365 calBCE (4665±30 BP, PSUAMS-2069)	Raschoille Cave, Oban, Argyll and Bute, Scotland	Great Britain
I3133	3631–3377 calBCE (4725±20 BP, PSUAMS-2154)	Raschoille Cave, Oban, Argyll and Bute, Scotland	Great Britain
I3134	3633–3377 calBCE (4730±25 BP, PSUAMS-2155)	Raschoille Cave, Oban, Argyll and Bute, Scotland	Great Britain
I3138	3263–2923 calBCE (4415±25 BP, PSUAMS-2156)	Raschoille Cave, Oban, Argyll and Bute, Scotland	Great Britain
I2610	1935–1745 calBCE (3515±35 BP, Poz-83498)	Summerhill, Blaydon, Tyne and Wear, England	Great Britain
I2634	3703–3534 calBCE (4851±34 BP, SUERC-68638)	Tulach an t'Sionnach, Highland, Scotland	Great Britain
I2635	3652–3389 calBCE (4796±37 BP, SUERC-68639)	Tulloch of Assery A, Highland, Scotland	Great Britain
I2633	3765–3641 calBCE (4911±32 BP, SUERC-68634)	Tulloch of Assery B, Highland, Scotland	Great Britain
I2453	2288–2040 calBCE (3760±35 BP, Poz-83404)	West Deeping, Lincolnshire, England	Great Britain
I2445	2136–1929 calBCE (3650±35 BP, Poz-83407)	Yarnton, Oxfordshire, England	Great Britain
I2447	2115–1910 calBCE (3625±25 BP, PSUAMS-2336)	Yarnton, Oxfordshire, England	Great Britain
I2786	2458–2205 calBCE (3850±35 BP, Poz-83639)	Szigetszentmiklós-Felső-Ürge hegyi dűlő	Hungary
I2787	2457–2201 calBCE (3840±35 BP, Poz-83640)	Szigetszentmiklós-Felső-Ürge hegyi dűlő	Hungary
I2741	2457–2153 calBCE (3835±35 BP, Poz-83641)	Szigetszentmiklós-Felső-Ürge hegyi dűlő	Hungary
I6531	2286–2038 calBCE (3755±35 BP, Poz-86947)	Dzielnica	Poland
I6579	2335–2046 calBCE (3780±35 BP, Poz-75954)	Iwiny	Poland
I6534	2456–2149 calBCE (3830±35 BP, Poz-75936)	Kornice	Poland
I6582	2343–2057 calBCE (3790±35 BP, Poz-75951)	Kornice	Poland
I4251	2431–2150 calBCE (3825±25 BP, PSUAMS-2321)	Samborzec 1	Poland
I4252	2285–2138 calBCE (3780±20 BP, PSUAMS-2338)	Samborzec 1	Poland
I4253	2456–2207 calBCE (3850±20 BP, PSUAMS-2339)	Samborzec 1	Poland
I6538	2008–1765 calBCE (3545±35 BP, Poz-86950)	Strachów	Poland
I6583	2289–2050 calBCE (3770±30 BP, Poz-65207)	Żerniki Wielkie	Poland
I4229	2288–2134 calBCE (3775±25 BP, PSUAMS-1750)	Cova da Moura	Portugal
I0462	2566–2345 calBCE (3950±26 BP, MAMS-25936)	Arroyal I, Burgos	Spain
I4247	2464–2210 calBCE (3870±30 BP, PSUAMS-2120)	Camino de las Yeseras, Madrid	Spain
I4245	2460–2291 calBCE (3875±20 BP, PSUAMS-2320)	Camino de las Yeseras, Madrid	Spain
I0257	2572–2348 calBCE (3965±29 BP, MAMS-25937)	Paris Street, Cerdanyola, Barcelona	Spain
I0825	2474–2298 calBCE (3915±29 BP, MAMS-25939)	Paris Street, Cerdanyola, Barcelona	Spain
I0826	2834–2482 calBCE (4051±28 BP, MAMS-25940)	Paris Street, Cerdanyola, Barcelona	Spain
I4068	2131–1951 calBCE (3655±20 BP, PSUAMS-2318)	De Tuithoorn, Oostwoud, Noord-Holland	The Netherlands
I4076	1882–1750 calBCE (3490±20 BP, PSUAMS-2319)	De Tuithoorn, Oostwoud, Noord-Holland	The Netherlands
I4075	2118–1937 calBCE (3635±20 BP, PSUAMS-2337)	De Tuithoorn, Oostwoud, Noord-Holland	The Netherlands